USGS
science for a changing world

Prepared in cooperation with the U.S. Army Corps of Engineers, New England District

Marine Geophysical Investigation of Selected Sites in Bridgeport Harbor, Connecticut, 2006

Scientific Investigations Report 2007–5119

U.S. Department of the Interior
U.S. Geological Survey

Cover. The Bridgeport Ferry heading toward Long Island Sound.

Marine Geophysical Investigation of Selected Sites in Bridgeport Harbor, Connecticut, 2006

By Carole D. Johnson and Eric A. White

Prepared in cooperation with the U.S. Army Corps of Engineers,
New England District

Scientific Investigations Report 2007–5119

U.S. Department of the Interior
U.S. Geological Survey

U.S. Department of the Interior
DIRK KEMPTHORNE, Secretary

U.S. Geological Survey
Mark D. Myers, Director

U.S. Geological Survey, Reston, Virginia: 2007

For more information on the USGS--the Federal source for science about the Earth, its natural and living resources, natural hazards, and the environment:
World Wide Web: http://www.usgs.gov
Telephone: 1-888-ASK-USGS

Suggested citation:
Johnson, C.D., and White, E.A., 2007, Marine geophysical investigation of selected sites in Bridgeport, Harbor, Connecticut, 2006: U. S. Geological Survey Scientific Investigations Report 2007–5119, 32 p., online only.

Contents

Figures

Table

Conversion Factors

Multiply	By	To obtain
	Length	
centimeter (cm)	0.3937	inch (in.)
meter (m)	3.281	foot (ft)
kilometer (km)	0.6214	mile (mi)
kilometer (km)	0.5400	mile, nautical (nmi)
	Weight	
kilogram (kg)	2.204	pound (lb)
	Speed	
meter per second (m/s)	3.281	foot per second (ft/s)

Temperature in degrees Celsius (°C) may be converted to degrees Fahrenheit (°F) as follows:

$$°F=(1.8×°C)+32$$

Horizontal coordinate information is referenced to the "North American Datum of 1983 (NAD 83)"

Altitude, as used in this report, refers to distance above the mean low-low water (MLLW).

Abbreviations

AGC	Automatic gain control
CAD	Confined aquatic disposal
CRP	Continuous resistivity profiling
CSP	Continuous seismic profiling
FM	Frequency modulated
GPS	Global positioning system
Hz	Hertz
kHz	Kilohertz
MLLW	Mean low-low water
min	Minute
ms	Millisecond
nT	NanoTesla
NOAA	National Oceanic and Atmospheric Administration
ohm-m	Ohm meter
PC	Personal computer
s	Second
TVG	Time variable gain
TWT	Two-way traveltime
USACE	U.S. Army Corps of Engineers
USGS	U.S. Geological Survey

Marine Geophysical Investigation of Selected Sites in Bridgeport Harbor, Connecticut, 2006

By Carole D. Johnson and Eric A. White

Abstract

A marine geophysical investigation was conducted in 2006 to help characterize the bottom and subbottom materials and extent of bedrock in selected areas of Bridgeport Harbor, Connecticut. The data will be used by the U.S. Army Corps of Engineers in the design of confined aquatic disposal (CAD) cells within the harbor to facilitate dredging of the harbor. Three water-based geophysical methods were used to evaluate the geometry and composition of subsurface materials: (1) continuous seismic profiling (CSP) methods provide the depth to water bottom, and when sufficient signal penetration can be achieved, delineate the depth to bedrock and subbottom materials; (2) continuous resistivity profiling (CRP) methods were used to define the electrical properties of the shallow subbottom, and to possibly determine the distribution of conductive materials, such as clay, and resistive materials, such as sand and bedrock; (3) and magnetometer data were used to identify conductive anomalies of anthropogenic sources, such as cables and metallic debris. All data points were located using global positioning systems (GPS), and the GPS data were used for real-time navigation.

The results of the CRP, CSP, and magnetometer data are consistent with the conceptual site model of a bedrock channel incised beneath the present day harbor. The channel appears to follow a north-northwest to south-southeast trend and is parallel to the Pequannock River. The seismic record and boring data indicate that under the channel, the depth to bedrock is as much as 42.7 meters (m) below mean low-low water (MLLW) in the dredged part of the harbor. The bedrock channel becomes shallower towards the shore, where bedrock outcrops have been mapped at land surface. CSP and CRP data were able to provide a discontinuous, but reasonable, trace from the channel toward the west under the proposed southwestern CAD cell. The data indicate a high amount of relief on the bedrock surface, as well as along the water bottom. Under the southwestern CAD cell, the sediments are only marginally thick enough for a CAD cell, at about 8 to 15 m in depth. Some of the profiles show small diffractions in the unconsolidated sediments, but no large-scale boulders or boulder fields were identified. No bedrock reflectors were imaged under the southeastern CAD cell, where core logs indicate the rock is as much as 30 m below MLLW.

The chirp frequency, tuned transducer, and boomer-plate CSP surveys were adversely affected by a highly reflective water bottom causing strong multiples in the seismic record and very limited depths of penetration. These multiples are attributed to entrapped gas (methane) in the sediments or to very hard bottom conditions. In a limited number of places, the bedrock surface was observed in the CSP record, creating a discontinuous and sporadic image of the bedrock surface. These interpretations generally matched core data at FP-03-10 and FB-06-1. Use of two analog CSP systems, the boomer plate and tuned transducer, did not overcome the reflections off the water bottom and did not improve the depth of penetration.

In general, the CRP profiles were used to corroborate the results of the CSP profiles. Relatively resistive zones associated with the locations of seismic reflections were interpreted as bedrock. The shape of the bedrock surface generally was similar in the CRP and CSP profiles. Evaluation of the CRP profiles indicated that the inversions were adversely affected where the depth and (or) ionic concentration of the water column varied. Consequently, the CRP profiles were broken into short intervals that extended just over the area of interest, where the depth to water bottom was fairly constant. Over these short profiles, efforts were made to evaluate the resistivity of the very shallow sediments to determine if there were any large contrasts in the resistivity of the sediments that might indicate differences in the shallow subbottom materials. No conclusions about the overburden lithology, however, can be drawn from the distribution of resistivity in the profiles.

A series of magnetic surveys also were conducted in Bridgeport Harbor. The magnetic data from Profiles 3, A, and B show a significant magnetic anomaly trending northeast and southwest. These anomalies indicate a possible large-scale feature that may be anthropogenic. Other isolated anomalies did not appear to be continuous or large scale. These features could be related to topographic changes (and changes in the height of the sensor above the bottom) or to metallic debris on the bottom or in the subbottom.

Introduction

The U.S. Army Corps of Engineers (USACE) is evaluating the feasibility of constructing confined aquatic disposal (CAD) cells associated with dredging in Bridgeport Harbor, Connecticut. Once a CAD cell boundary is established, the native materials within the CAD cell are excavated for off-site removal, leaving the CAD cell available to receive dredged material removed from the Federal navigation channel. Borings, including coreholes and probes, collected at the site indicate a highly variable bedrock surface overlain by varying amounts of till, sand, fine sand, and organic deposits (U.S. Army Corps of Engineers, written commun., 2006). In cooperation with the USACE, the U.S. Geological Survey (USGS) collected continuous seismic profiling (CSP), continuous resistivity profiling (CRP), and magnetometer data in Bridgeport Harbor. The geophysical data will be used by the USACE to help identify the location and potential capacity of CAD cells.

The optimal CAD cell location would have at least 30 m of sediments above the bedrock, be free of boulders, cables, pipes, and large debris that might hamper excavation, and be outside the shipping channel. The CAD cell would contain easy-to-excavate clean sand and near-surface clays that could be used to top off a completed CAD cell. A minimum depth of 15 m of sediments is needed for a "starter cell" that can be used in tandem with another cell to hold materials that are unsuitable in the construction and completion of the other CAD cell.

Initially, the USACE chose to evaluate two locations in the harbor (fig. 1A). The northern potential CAD cell site proved to have a substantial amount of silt considered unsuitable for ocean placement, which made CAD cell development at that location unfeasible (U.S. Army Corps of Engineers, written commun., 2006). A possible CAD cell site in the southwestern part of the harbor outside of the navigation channel also was identified. Results of field explorations indicated that because of the shallow depth to bedrock under this site, it did not have the capacity to meet the project needs alone. For that reason, a new CAD cell site was added to the southeastern part of the harbor (fig. 1A).

From April 7 to 14, 2006, CSP, CRP, and magnetometer data were collected along seven profiles in Bridgeport Harbor. Profiles 1 to 5 were part of the initial plan for surveying the harbor. During the field operation, Profiles A and B were added to help characterize the location of the proposed southwestern CAD cell. The proposed northern CAD cell, surveyed with Profiles 4 and 5, became less favored than the southwestern CAD cell because of the depth of silt material located over the parent material. Although CRP and CSP data were collected for Profiles 4 and 5, their interpretations were postponed, while Profiles A and B, over the southwestern CAD cell, were given a higher priority for completion than data collected over the northern CAD cell. After preliminary data interpretation and results of the drilling program in the harbor, the sizes of the CAD cells were modified to smaller footprints (fig. 1A).

A secondary pilot investigation was conducted from October 10 to 11, 2006, to evaluate different seismic sources at the third proposed CAD cell on the southeastern side of the harbor. These sound sources included analog, boomer-plate, and tuned transducer sources that were compared to the chirp or swept-frequency source. Analog sound sources were used in Profiles D, E, and F over a third proposed CAD cell on the southeastern side of the harbor.

Purpose and Scope

The purpose of this report is to describe the marine geophysical methods used in the 2006 investigation of Bridgeport Harbor. The report also provides interpretation of the geophysical data; compares the results to the local geology; correlates the geophysical data with drilling and coring data; and discusses the effectiveness of each geophysical method for this application. The report provides an example of using a multi-method approach for characterizing the subsurface beneath the water. The investigation shows the importance of having good control data, such as boreholes in order to constrain the inversion and inform the processing and interpretation of the geophysical data.

Description of the Study Area

Bridgeport Harbor is located approximately 30 km north of the New York-Connecticut state line. It is an active harbor, with multiple docks and industries, and accommodates the ferry that goes to Port Jefferson on Long Island. Three tributaries empty into the harbor—the Pequannock River, Yellow Mill Channel, and Johnson's Creek (fig. 1B). Core samples collected over the proposed CAD cell locations showed a layer of muck and organic sediments over unconsolidated sediments of coarse to fine material that were deposited on schist (U.S. Army Corps of Engineers, written commun., 2006). Parts of Bridgeport Harbor are as much as 18 m deep, and the shipping channel is dredged to a depth of as much as 40 m. The tide changes more than 2 m per day, so it was important to access the shallowest locations near the shorelines when the tide was high. Also, it was essential to correct all data collected for this investigation to a common datum, such as the mean-low-low water (MLLW) level.

Methods of Data Collection and Analysis

Three water-based geophysical methods were used to evaluate the subsurface materials in Bridgeport Harbor—CSP, CRP, and marine magnetometer. All data points were located

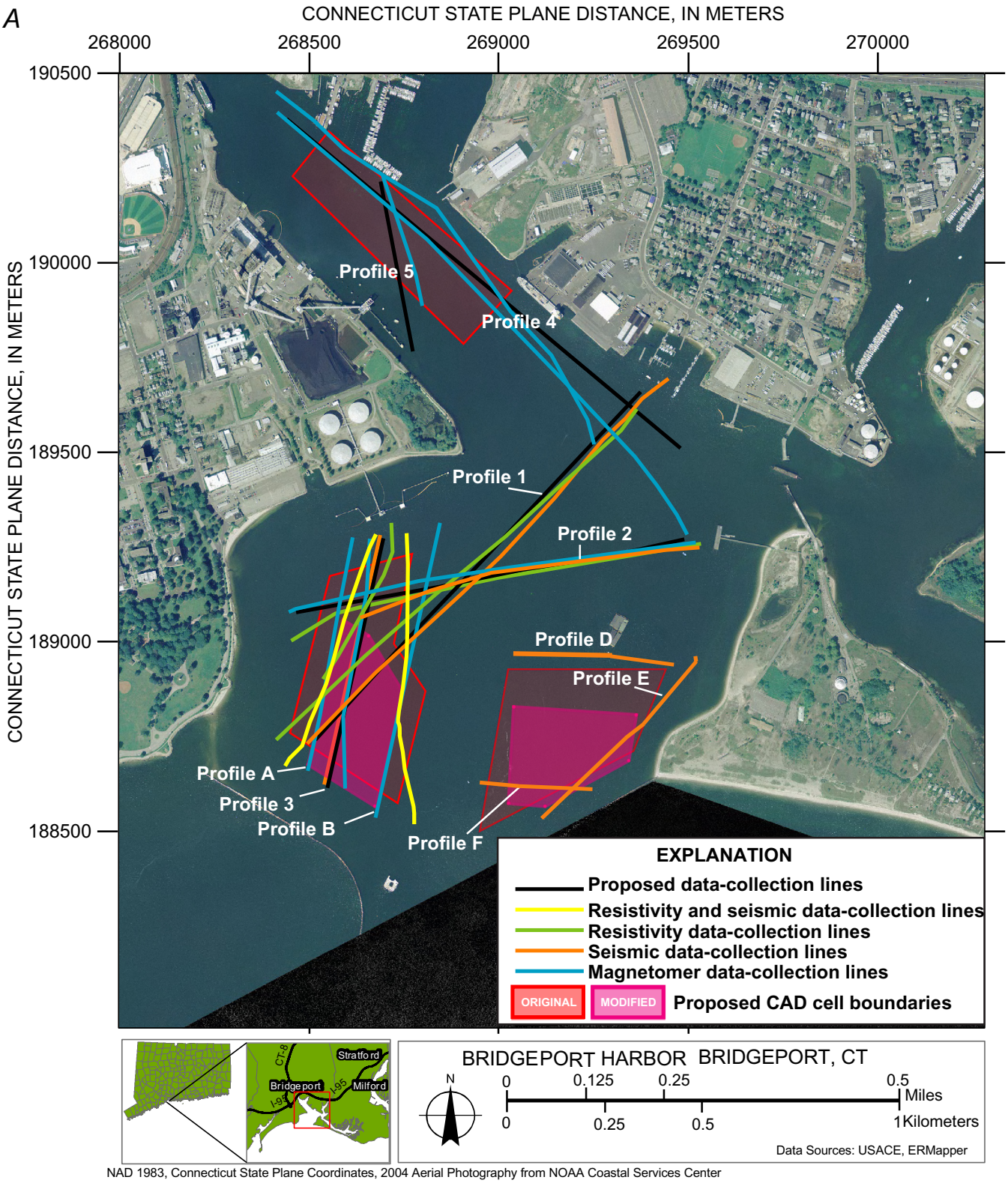

Figure 1. (*A*) Bridgeport Harbor, Bridgeport, Connecticut, showing profiles along which data were collected.

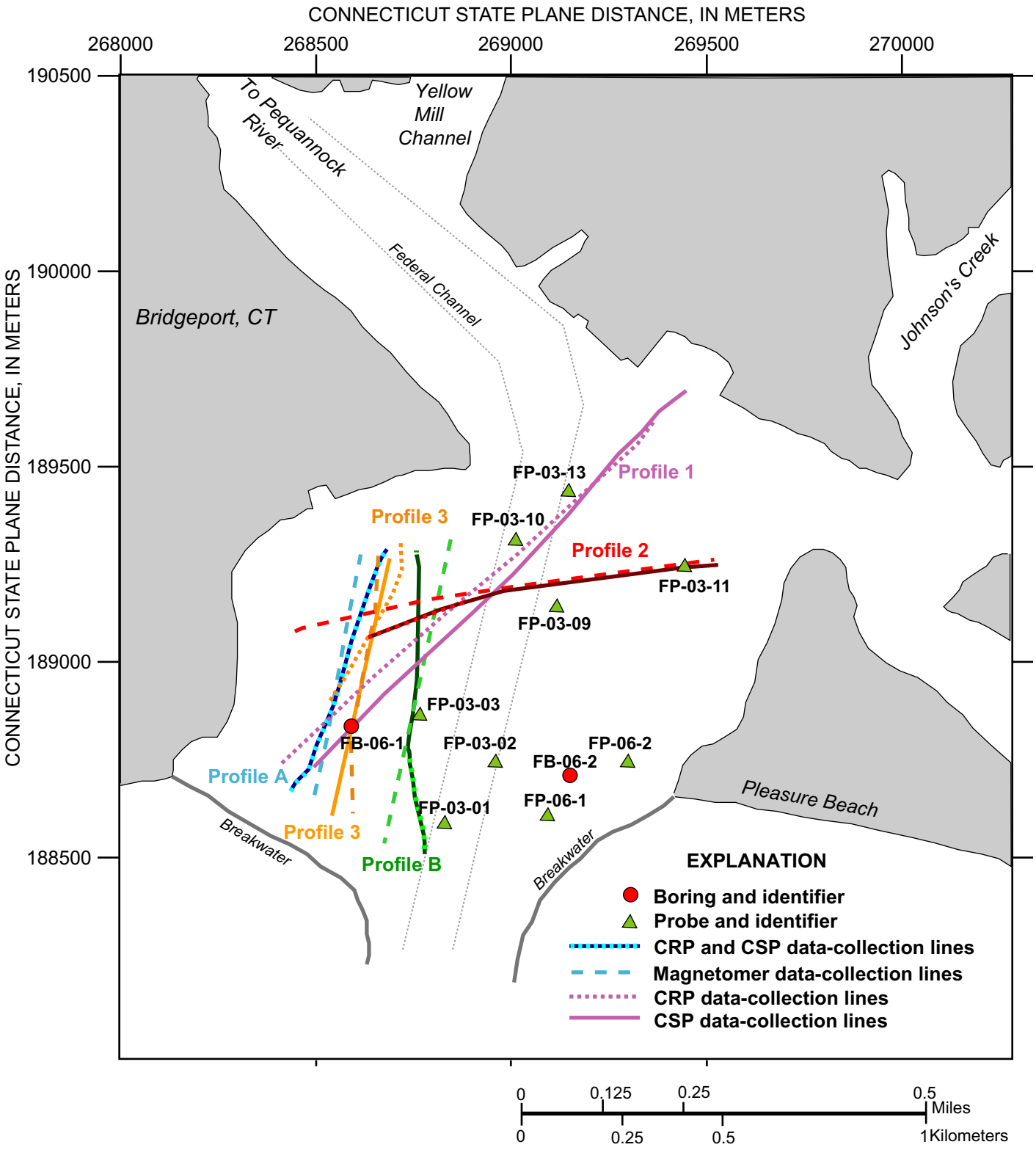

Figure 1. (*B*) Selected geophysical profiles, borings, and probe locations in Bridgeport Harbor, Bridgeport, Connecticut. All surveys for a single profile are shown in the same line color and the survey type is indicated by the line type. CRP is continuous resistivity profiling; CSP is continuous seismic profiling.

using global positioning systems (GPS), and GPS data were used for real-time navigation to follow predetermined profile locations. During data collection, CSP and CRP locations were compared to locations of existing core information, and the profile locations were mapped in real time and plotted on a digital georeferenced map. The real-time plotting was helpful for evaluating the ship's position relative to the proposed lines in the scope of work, the existing data, and possible sources of side echoes in the seismic data.

All data were inspected in the field and preliminary interpretations were conducted to evaluate the adequacy of the data-collection methods. When possible, field observations were used to help interpret the data in real time, including observation of water bottom, shoreline, piers, and the breakwater. The CRP data were difficult to assess during data collection because the data must be postprocessed and inverted in order to interpret the data; the ship's navigational track, however, was evaluated in real-time.

Navigation

Navigation data for the CSP and magnetometer surveys were collected with a Trimble GPS in WGS84 and were passed to the acquisition software and the navigational software at a rate of once per second. DelphMap software, was used to plot the course of the boat and allow real-time navigation along cruise lines predetermined by the USACE. Each profile was plotted on an image of the harbor, so that the boat driver could navigate along the cruise lines during data collection.

Prior to the use of GPS technology for navigation and positioning, a commonly used approach was to maintain a constant boat speed during data collection between two known points. In postprocessing, the geophysical profile was fit between the known points along the line. This rubber-sheeting method was used for interpretation of the Profile 3 data, because the GPS data for Profile 3 were corrupted. Hence, all points along Profile 3 were incrementally positioned along a straight line between the two end points.

Although CRP and navigation data were collected concurrently, the data were collected with independent software and equipment. A hand-held Lowrance LMS480 was used to obtain GPS data, depth to water bottom, and water temperature. The GPS and associated data were captured in HyperTerminal software and stored digitally. The GPS data were synchronized with the CRP data in postprocessing.

Tidal Stage

Tidal stage data for Bridgeport Harbor were obtained from verified tidal records from the Bridgeport Harbor, Connecticut, Station 8467150 maintained by the National Oceanographic and Atmospheric Administration (NOAA). The tidal levels were reported at 6-min intervals (fig. 2). The MLLW was determined for each of the profiles using the times listed in table 1. A correction factor was applied to all interpreted data listed in the table; the original data plots, however, remain relative to the ambient water level at the time of collection.

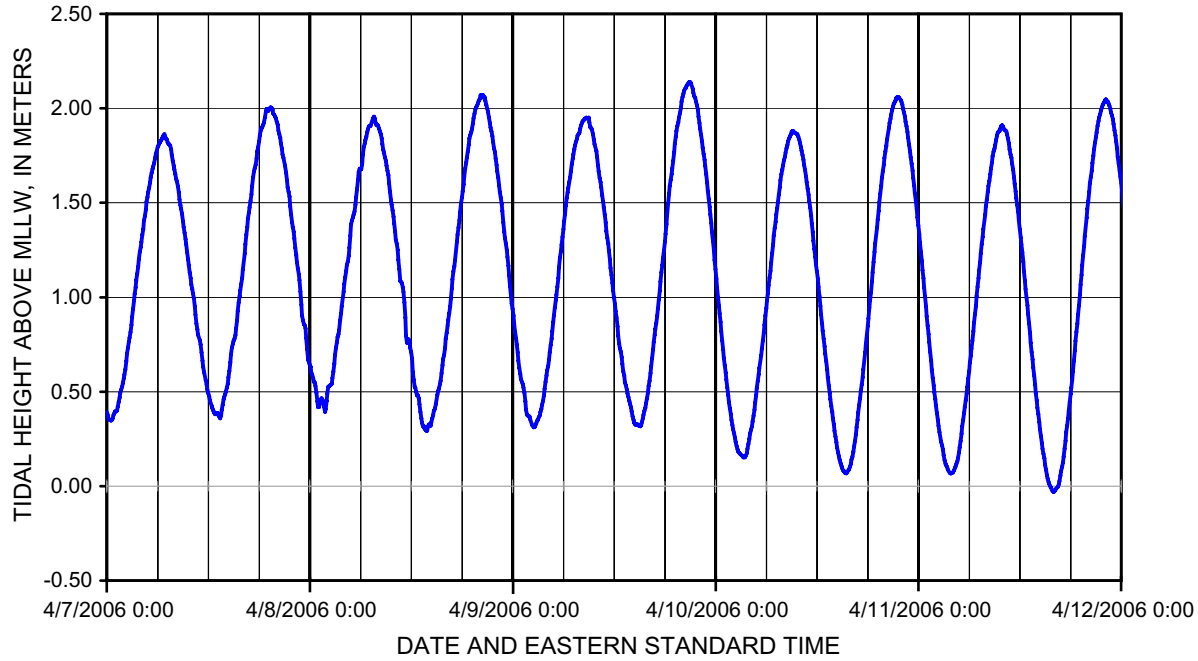

Figure 2. Tidal levels at Bridgeport Harbor, Bridgeport, Connecticut. Tidal measurements were taken from Bridgeport Harbor Station 8467150. Tidal heights are shown in meters above mean low-low water (MLLW).

Table 1. CSP and CRP profiles collected in Bridgeport Harbor, Connecticut, April 2006.

[CSP, continuous seismic profiling; CRP, continuous resistivity profiling; GMT, Greenwich Mean Time; EST, Eastern Standard Time; MLLW, mean low-low water; SW, southwest; NE, northeast; E, east; W, west; N, north; S, south; SE, southeast; NW, northwest]

Profile	Date collected	Time collected GMT	Time collected EST	Water level relative to MLLW (meters)	Water level relative to MLLW (feet)	Direction of original profile
CSP 1	4/7/2006	17:56	13:56	0.49	1.60	SW to NE
CRP 1	4/10/2006	16:36	12:36	0.86	2.83	SW to NE
CSP 2	4/7/2006	18:19	14:19	0.54	1.78	E to W
CRP-2	4/10/2006	17:20	13:20	0.55	1.80	E to W
CSP 3	4/11/2006	16:53	12:53	0.96	3.14	N to S
CRP-3	4/10/2006	18:00	14:00	0.33	1.07	N to S
CSP-A	4/12/2006	15:50	11:50	1.77	5.80	N to S
CSP-A concurrent with CRP	4/12/2006	19:09	15:09	0.27	0.89	N to S
CRP-A	4/12/2006	19:08	15:08	0.27	0.89	N to S
CSP-B	4/12/2006	16:16	12:16	1.52	5.00	N to S
CSP-B concurrent with CRP	4/12/2006	19:16	15:16	0.21	0.70	N to S
CRP-B	4/12/2006	19:18	15:18	0.21	0.70	N to S
CSP-4	4/11/2006	17:35	13:35	0.63	2.06	SE to NW
CRP-4	4/10/2006	16:58	12:58	0.72	2.35	
CSP-5	4/11/2006	17:44	12:44	1.04	3.42	NW to SE
CRP-5	4/10/2006	17:45	13:45	0.41	1.35	

Continuous Seismic Profiling (CSP)

A single-channel seismic reflection system consists of a sound source, receiver, and recording system. A sound wave is transmitted through the water column and into the underlying sediments. The sound waves are reflected off reflectors on the bottom and in the subbottom and are detected by one or more receivers on or near the water surface. The two-way traveltime (TWT) of the seismic wave is recorded and stored. Using an assumed velocity of the sound wave in water and saturated sediments, the depth to the reflector can be estimated.

Theory of CSP

Understanding the basic principles of seismic theory is necessary for choosing the correct equipment for the field application and for interpreting the CSP data. The velocity of a sound wave is proportional to elastic properties and inversely proportional to the density of the medium through which it travels (Trabant, 1984). The seismic data consist of a series of traces showing the amplitude of the reflections as a function of traveltime. Plotted side by side, the trace data appear as a cross section of the subbottom under the survey line. Within the seismic cross section, diffractions and reflections can be traced, characterized, and correlated with geologic cross sections.

This section reviews how seismic reflections are produced and describes the basics of seismic theory and CSP interpretation. The resolution of the seismic method is a function of both the compressional seismic velocity of the material and the frequency of the wave. As a seismic wave propagates through a medium, energy is lost by spreading, reflection, scattering, and absorption of the wave. The energy loss is proportional to the wave frequency. High frequency waves are attenuated more readily than low frequency waves, so low frequency waves travel further than high frequency waves. Although lower frequencies can provide an increased depth of penetration, they have a lower resolution than higher frequency signals. At higher frequencies, there is greater resolution or increased ability to resolve smaller features, but at the expense of the depth of penetration.

Reflections of seismic energy occur at the interface of two materials with differing acoustic impedance:

$$Z = \rho V , \tag{1}$$

where

Z is acoustic impedance [in units of mass/length^2 time],

ρ is density [mass/length^3],

and

V is velocity of sound through the medium [length/time].

Because the densities of subbottom materials generally are similar, reflections occur mostly because of changes in the velocity of sound through the materials.

The strength of the reflected signal, the reflection coefficient, is proportional to the ratio of amplitude of the reflected wave to the amplitude of the incident wave, which is a function of the difference in acoustic impedance of the two media. The higher the contrast in acoustic impedance between the two media, the stronger the reflection coefficient. The reflection coefficient is defined as

$$RC = A_r/A_i = (Z_2 - Z_1)/(Z_2 + Z_1) , \tag{2}$$

where

RC is the reflection coefficient,

A_r is the amplitude of the reflected wave,

A_i is the amplitude of the incident wave,

Z_1 is the acoustic impedance of layer 1,

and

Z_2 is the acoustic impedance of layer 2.

Examples of $RC = (\rho_2 V_2 - \rho_1 V_1) / (\rho_2 V_2 + \rho_1 V_1)$, where ρ_1 and ρ_2 are the density, and V_1 and V_2 are the velocity of sound, in layers 1 and 2, above and below the interface, respectively, are

Water to air = -1 (the negative sign indicates the reflection is out of phase with the incident signal)

Water to mud	= 0.05 to 0.1
Mud to clay or silt	= 0.1
Water to clay/ silt	= 0.1
Water to sand	= 0.3 to 0.4
Sand to bedrock	= 0.5 to 0.7
Water to bedrock	= 0.7 to 0.8

These values indicate water-to-air and water-to-bedrock interfaces would have very strong reflections, whereas water-to-mud or mud-to-sediments interfaces would have fairly weak reflections.

In order to image subsurface layers, there must be (1) transmission of energy into the subsurface, (2) a high enough frequency of energy to resolve the layer, and (3) sufficient contrast in velocity and density (acoustic impedance) between the media to cause a reflection at the interface. Consequently, if there is a strong reflection off of an interface, then much or all of the signal is reflected and little or no signal propagates deeper into the subbottom. The lower the contrast in the acoustic impedance, the more likely the seismic signal is transmitted through the layer interface without reflections.

Linear or point reflectors are identified in the seismic trace data. With the seismic trace data plotted side-by-side, reflections are identified and interpreted as side echoes, water bottom, boulders, or bedrock surface. Reflection patterns also can be used to characterize and interpret subbottom materials. For example, layered, continuous, and coherent patterns may indicate layered sediments, whereas chaotic, discontinuous, or diffracted patterns might indicate coarse, poorly sorted deposits, till, and (or) boulders.

Equipment and Methods of CSP Data Collection

In general, a CSP system consists of a sound source, receiver, personal computer (PC), monitor, and control unit that amplifies the outgoing sound wave, processes the incoming pulse, and passes the digital data to the hard drive and monitor. Typically, a generator is required to power all of the onboard and submerged equipment. Seismic reflection profiles were collected on a WindowsXP computer using SB-Logger acquisition software, produced by Triton Imaging, Inc. SB-Logger was run in real-time recording mode and was used with a topside unit (control unit) and towfish manufactured by EdgeTech. The sound source used for this investigation was a swept frequency, or chirp, system that sweeps through a range of frequencies from low to high. Chirp, which is an acronym for compressed high intensity radar pulse, originated in the field of airborne radar technology, and has been applied in the field of seismic imaging.

Two towfish were used for this investigation (figs. 3A, 3B, 3C). Each towfish is a self-contained unit that houses a chirp seismic source and two receivers. For each towfish the reflected acoustic signal was received by the transducer, converted to an electrical signal, and transmitted to the control unit where it could be amplified, processed, stored digitally, and displayed on a monitor.

The lower frequency towfish, the SB-0512i, was used first to assure the depth of penetration was achieved. The transmitting transducer in the SB-0512i sweeps through a specified range of frequencies within the band of 500 Hz to 12 kHz. The SB-0512i towfish is approximately 1.8 m long, and weighs 200 kg in air and 160 kg submerged. For this application, the antenna was tethered to its own catamaran and was submerged about 1 m below water surface.

The higher frequency towfish used was an EdgeTech SB-216s. The transmitting transducer in the SB-216s sweeps through a range of frequencies including 2 to 10, 2 to 12, and 2 to 16 kHz. The SB-216s is approximately 1 m long, weighs 70 kg in air and 45 kg submerged. For this application, it was towed tethered to the boat and submerged about 1 m below water surface (fig. 3A).

To decrease the propagation losses and to improve resolution of the reflectors, the energy of the outgoing pulse was adjusted for each towfish. An increase in power may or may not improve the resolution, so a trial-and-error approach was used. In general, setting the power at about 80–90 percent of full scale maximized the signal-to-noise ratio. In the presence of strong water-bottom multiples, the optimal power setting was a lower value.

The chirp acoustic sources use a digitally generated, frequency modulated (FM) pulse that sweeps over a user-specified frequency range. The chirp data shown in this report were collected with Triton Imaging SBLogger software. For this investigation, two transmission ranges were used, 500 Hz to 6.2 kHz and 2 to 10 kHz, over a 40-ms interval. Time-sampling intervals were determined by data quality during acquisition. Transmission was typically 2 or 4 times per second, and the recording length was 100 ms, which is approximately equivalent to a depth of 75 m in water and sediments. The hydrophone arrays in the towfish are omni-directional receivers that are used to measure the incoming or returned pulse. With a chirp system, the returned multiplexed signal is processed in a form of cross-correlation with the transmitted signal (Trabant, 1984). For the chirp antennas, the output signal is received by the data control unit, which performs a correlation of the output signal with a proprietary pulse (that is a function of the output pulse frequency band); the resulting signal is then stored as data in SEG-Y format (Schock and LeBlanc, 1990).

In addition to the digital chirp sound sources, two analog sources (a boomer plate and a tuned transducer) were used in the second phase of the investigation when seismic lines were collected on the southeastern side of the harbor to evaluate another potential CAD cell. The analog sources were used to test different types of sound sources in efforts to get better records than were obtained with the chirp equipment. In fine sands, silts, and clay materials, chirp and boomer-plate systems can achieve equal depths of penetration, provided they are not attenuated on an acoustically hard water bottom. In coarse sands, a boomer plate can achieve greater depths of penetration than the chirp signal. Data from both methods, however, are subject to interference from strong multiples produced by acoustically hard water bottoms.

The Geopulse boomer plate (fig. 3D) is an electro-mechanical sound source that produces a low-frequency, broad-band sound source (Haeni, 1986). Two spring-loaded plates in the antenna are electrically charged, causing them to repel one another and the plates to spread apart; when the charge is dissipated, the plates clap back together producing the acoustic signal. The boomer plate is mounted on a rigid catamaran and towed behind the boat (fig. 3D). The outgoing frequency of the boomer equipment was measured with a calibrated hydrophone, and ranged from 200 to 1,200 Hz (a 1-kHz bandwidth) with maximum peak energy at about 700 Hz. A partially submerged hydrophone or streamer is used with the boomer-plate system to record the seismic wave arrivals. In a single-channel array, a number of hydrophones are linked together to provide a single channel response; multi-channel methods collect the offset arrivals of a signal along the streamer. Multi-channel methods require complex processing and analysis and were not used in this study.

Tuned transducers, or "pingers," consist of a transducer and a receiver (fig. 3E). These "tuned" sound sources have a narrow bandwidth with specific center frequencies. Using a calibrated hydrophone, the outgoing frequency was measured, and the frequency content of the pinger used in this study was verified to be centered at 3.5 kHz.

The boomer plate and tuned transducer (analog) data presented in this report were collected with Delph Seismic acquisition software. The data passed through a preamp on the streamer and were then filtered and amplified at the receiver box. Then, the data were passed to a PC with an

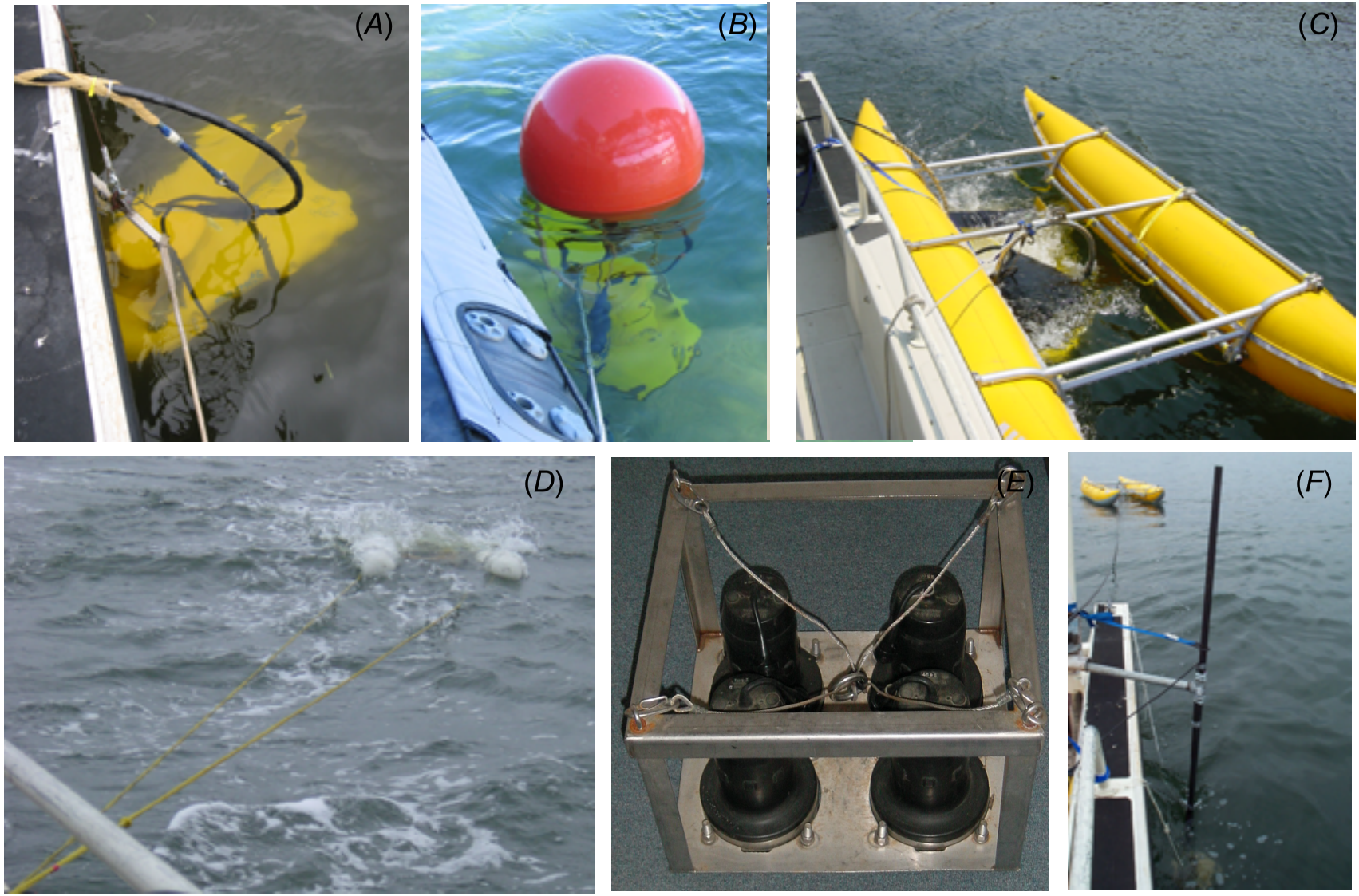

Figure 3. Seismic sound sources used at Bridgeport Harbor, Connecticut, including (*A* and *B*) a swept-frequency SB-216s towfish tethered to the boat and towed with a buoy; (*C*) a SB-0512i towfish with a catamaran; (*D*) a boomer plate towed behind the boat on a catamaran; (*E*) 3.5- and 7-kilohertz-tuned transducers; and (*F*) a high frequency echo sounder (the SB-0512i towfish is in the distance). All sound sources are recorded digitally.

analog-to-digital board and were stored digitally in SEG-Y format. During data acquisition, various ranges of band-pass filter settings were applied at the receiver box to strip out the high-frequency side-echo data and low-frequency noise to optimize the seismic record. In addition, data were collected in raw form and filtered in postprocessing.

A high-frequency echo sounder was used to map the water bottom during seismic surveys. Shown in the foreground of figure 3E, the HydroTrac 200-kHz single-beam echo sounder provided high resolution water-bottom data. This echo sounder has a manufacturer's reported resolution of 3 cm. These data also can be used to monitor the water depth in real-time for navigation.

Limitations to CSP Data Collection

Navigation, access, safe passage through the study area, and sufficient water depth were limitations that hampered data collection. Limitations on the quality of the data include hard water-bottom reflectors and entrapped gas in the sediments. Hard water bottoms can reflect much of the signal, preventing penetration of the signal to the subsurface. Seismically hard water bottoms are comprised of cobbles, boulders, or hard-packed sediments. Additionally, organic material rich in entrapped gas can prevent signal penetration and cause multiple reflections. Because of the strength of the reflection of a water-bottom multiple, more subtle features in the seismic record often are obscured.

Limitations of the single-channel boomer plate and streamer systems include misalignment of the sound source and receivers. Alignment is a problem when space is limited and the vessel has to make several tight turns or when there are strong currents that continually move the streamer relative to the source, or push the streamer toward the outboard motor. In these cases, the single-body towfish has advantages over the boomer-plate and streamer systems.

Interpretation of CSP data

Postprocessing to display and interpret the chirp data shown in this report was done in SBInterpreter and ReflexW software packages. The interpretation software was used to independently view the real and imaginary signals and the envelopes of the real and imaginary signals, and to interpret reflectors in the seismic trace data. For this investigation, the interpretation relied primarily on the envelope data. Depth to water bottom and subbottom stratigraphic variation were determined where possible.

The analog data were displayed and interpreted in SB Interpreter where filters and gains were applied to enhance the images. A band-pass filter, which allows frequencies to pass through a specified window, was used to remove unwanted frequencies that obscure possible subbottom reflectors. The band-pass filter had a high-pass filter set at 4.8 kHz and a low-pass filter set at 2.5 kHz. To help reduce the presence of electrical noise and boost the signal, the data were filtered using a 60-Hz notch filter, which rejects the frequencies within a specified band, and were gained using an automatic gain control (AGC) and time-varying gain control (TVG). The AGC uses an algorithm that adjusts the mean absolute signal value to the cumulative mean absolute value signal for all previous traces. TVG improves the profile appearance by correcting for attenuation of the acoustic signal caused by spherical spreading and then computes an adjusted signal value.

The CSP profiles were plotted in the most optimal color schemes and scales to enhance subtle features and facilitate interpretation. This was done on a trial-and-error basis for each profile. With the most enhanced colors and gain settings, reflectors were identified in the seismic profiles and digitized. Features observed in the CSP record include side echoes, multiples, water bottom, and subbottom reflections.

Side echoes are high-frequency reflections off solid features in the water, such as piers, buoys, breakwaters, and shorelines. Side echoes typically have a high-frequency signal and can sometimes be filtered out with low-pass or band-pass filters. Filters are not applied to chirp data, because it is not recommended with the signal processing that is built in to the data control unit (Robert Morris, Edgetech, oral commun., 2006). The locations of side echoes can be verified in the field by observing the reflector and moving towards or away from the object while comparing the reflection with the distance between the antenna and the object. In this investigation, no intended diversions were taken off the predetermined profiles, but the sources of potential side echoes were noted in the field and the geometry of the reflectors was checked against the navigational data and map images.

Water-bottom multiples are the result of the outgoing seismic signal reflecting back and forth between an acoustically hard bottom and the water surface. A classic feature of the multiple is that the slope in the reflected multiple increases as the multiplicity of the reflection increases. Two major problems with multiples are that (1) the reflections obscure the real subbottom reflectors and (2) much of the seismic energy is reflected at the hard bottom and little or no signal penetrates to the subbottom.

Reflections off of boulders, cobbles, and pipes can cause point reflections that appear as diffractions. Coarse-grained deposits tend to have diffractions and chaotic reflections.

Subbottom reflections off sedimentary layers or at the interface with the bedrock surface appear as low amplitude reflections. They can be continuous or discontinuous reflectors. Subbottom reflections typically have lower amplitude and lower frequency than the side and water-bottom reflections, but it is important to differentiate them from any water-bottom multiples.

Reflectors were picked in the display and interpretation software package. The georeferenced coordinates and depth to the reflector were exported as x, y, z data in ASCII format, where x and y are easting and northing, in meters, and z is two-way traveltime, in milliseconds. The results

were imported into Excel, where the x and y location data were converted to feet, and the distance along the line was computed and recorded in feet. In addition, the TWT was converted to meters (and feet) below water surface, using an assumed velocity of 1,534 m/s, to determine the depth to the reflector below the antenna and a correction for the distance from the bottom of the transmitter to the water surface (Telford and others, 1990). The velocity of sound in water varies according to temperature and salinity of the water (Mackenzie, 1981). Changes in the depth of reflectors due to the range of values of velocity are estimated to be ± 3 percent. Computing depths for the water column and the saturated sediments using unique velocities for each of the media, (1) requires good control data for the depths to reflectors to estimate those velocities and (2) produces very small differences in the estimates of the depth to bedrock. Without better estimates for the saturated sediments, a uniform velocity was used for both the water and the saturated sediments. All estimated depths should be considered to be ±10 percent (F. P. Haeni, U.S. Geological Survey, retired, oral commun., 2007). For reporting purposes, the depths to the reflectors were adjusted to the MLLW surface as a common datum between surveys.

In addition, the TWT for the water-bottom multiples were calculated and plotted along with the interpreted reflectors over the seismic record in depth below the ambient water level. The composite plot allowed differentiation of reflectors and multiples, thus avoiding erroneous interpretations of the bedrock surface. The profiles were interpreted more than once to test the repeatability of the interpretation. The interpretations of reflectors also were correlated to drilling records and to tie-line crossings where profiles crossed. All interpreted depths to bedrock were summarized in tables in units of feet and made available to the USACE. In this report, all data are reported in metric units and original data plots not corrected to MLLW. The plots are shown with the depth below the antenna, which is 1 m below the water surface. The text refers to the depth in terms of meters below the ambient water level (as shown on the plots) and from MLLW.

Continuous Resistivity Profiling (CRP)

CRP makes use of the principle that subsurface resistivity is affected by the composition of the subsurface materials, the amount of water-filled pores, and the ionic concentration of the fluids in the pore water. The CRP method was used to help corroborate the depth to bedrock determined with the CSP and potentially determine the type of sedimentary materials in the subsurface in the area of the proposed CAD cells.

Theory of CRP

The theory behind CRP is similar to that for land-based two-dimensional (2D) electrical resistivity profiling. An electrical current is injected through two current electrodes into the surrounding water and subbottom, and voltage differences are measured across pairs of potential electrodes. The apparent resistivity of the water and subsurface is determined from the potential voltage measurements by using Ohm's Law and applying a geometric correction for the specific array geometry:

$$\rho_a = k \Delta V / I \ , \qquad (3)$$

where

ρ_a is the computed apparent resistivity;

k is the geometric factor depending on the configuration of the survey array, which for dipole-dipole surveys, $k = \pi\, n\, (n+1)\, (n+2) a$; a is the electrode spacing; n is the ratio of the distance between the current electrodes plus the distance between the current and potential electrodes to the electrode spacing, which in this array is equal to the measurement number;

ΔV is the measured potential difference;

and

I is the injected current.

The apparent resistivity is plotted in a pseudo-section in which the data are displayed such that the horizontal position is the midpoint distance between electrode pairs and the vertical placement is a function of the separation distance (fig. 4). The pseudo-depth is computed as the intersection of 45° angles from the midpoint of the electrode pairs or as the Frechet derivative for a homogeneous half space (Loke, 2001).

The obvious difference between the application of marine and land-based resistivity is that in the water, the electrodes in the streamer are coupled directly with the water and measurements are taken continuously as the electrode array is advanced through the water. The dipole-dipole array is ideal for water-based applications, because of the geometry and the speed in data collection, which is important for a slow-moving array. Although the dipole-dipole array provides a more rapid rate of data acquisition and higher resolution of subsurface features, compared to Schlumberger or Wenner configurations, the signal and the depth of penetration are weaker than for these other configurations (Ward, 1990).

The distribution of resistivity is interpreted for water, sedimentary materials, or bedrock. The calculation for apparent resistivity data assumes the earth is homogeneous and isotropic. True resistivity is estimated by inversion of the calculated apparent resistivity of the measured field data. The inversion process seeks to determine a subsurface model response that best matches the measured data with certain constraints. The initial inverse model is modified with each iteration in an effort to minimize the differences in the computed model and the observed data. In most programs this is done by comparing simulated apparent resistivity section with the apparent resistivity section of the observed data. The process is continued until the difference in the model is minimized to within a user-specified tolerance.

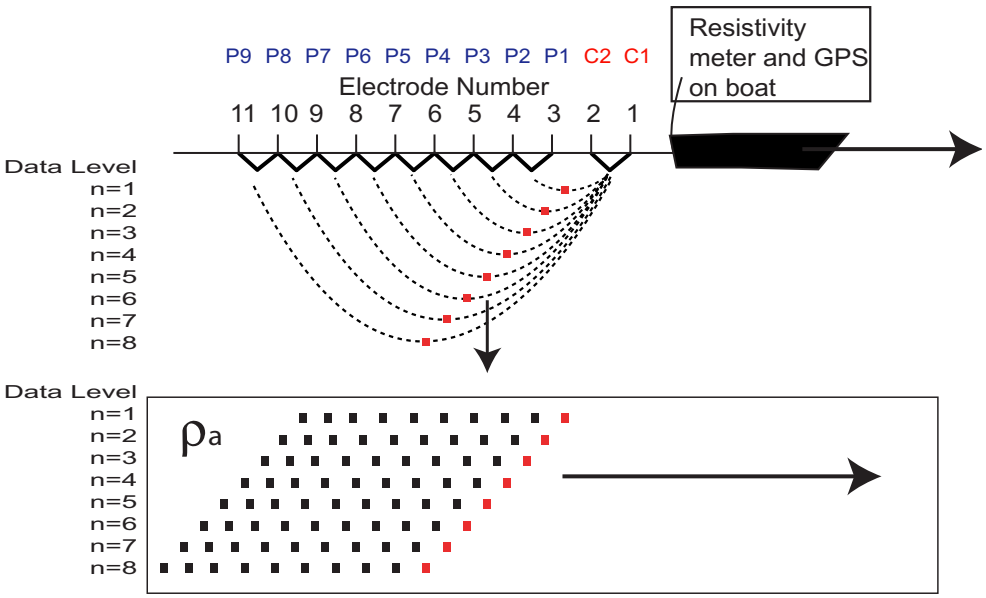

Figure 4. Array geometry of a continuous resistivity profile dipole-dipole survey and the measurement locations. C1 and C2 are the current electrodes, P1, ... P9 are the potential electrodes, and ρa is the apparent resistivity of the medium, shown in a pseudo-section.

.

Equipment and Methods of CRP Data Collection

Boat navigation was monitored using GPS and navigational software that plotted the course of the boat in real time. The boat speed was approximately 1.2 m/s (2.5 knots).

An 8-channel, 200-watt Advanced Geosciences, Inc. Super Sting was used to collect the CRP data. For this investigation, 11 electrodes spaced 10 m apart and mounted in a streamer were towed behind the boat. The first two electrodes, closest to the boat, were used to inject current into the water and subbottom materials, and eight electrical potential measurements were made using the remaining nine electrodes. With this system, a complete suite of dipole-dipole measurements is collected every 2.8 s. Because the boat is moving at a slow rate of speed, a complete measurement is taken while the boat has moved about 3.4 m. Although subbottom conditions probably do not change much over this short interval, there is insufficient time to collect reciprocal data or to stack the signal during data collection, as is frequently done in land surveys. Also, unlike typical land surveys, only the first electrode pair is used to transmit current. An apparent resistivity value is generated for each potential measurement pair, and is schematically shown as the midpoint between the current and potential electrode pairs (fig. 4). With this equipment and approach, approximately 4 km of CRP data can be collected in an hour.

Limitations of CRP Methods

One of the limitations of the marine CRP method is that the current is dissipated in the water; thus, only short electrode spacings (relative to land-based surveys) can be used. The depth of investigation is a function of water column and subsurface resistivity and array geometry including the array type and electrode spacing. The maximum depth of penetration of a resistivity measurement is proportional to the electrode spacing and inversely proportional to subsurface conductivity (Edwards, 1977). With electrode spacings of 10 m, the electric signal penetrates about 25 m or less, and with electrode spacings of 5 m, penetration is limited to about 11 m. With array spacings greater than 10 m, the electric signal probably would not penetrate the subsurface because the signal voltage levels decline significantly with increased array spacing.

Sources of error in measurements are random noise, poor electrode alignment, and (or) poor electrode coupling due to cavitation. Sources of error in the inversion include overfitting, or underfitting data relative to the actual noise level; errors resulting from the finite-difference approximation and assumed boundary conditions; and the assumption of 2D homogeneity, that is, no variability perpendicular to the CRP track. Overfitting and underfitting data arise, respectively, from matching data better or worse than warranted

by measurement errors. In CRP, reciprocal and repeat measurements are commonly unavailable, so there is less information for selection of the number of iterations or target error (root mean squared or absolute) than for land-based resistivity measurements.

Sources of error in the interpretation include the errors in the inversion, the assumption of two dimensions, and the choice of boundary conditions for the inversion. Because of the increased data density and survey geometry, there is greater resolution and certainty in results from the middle of the survey line and from shallow depths than in results from the ends of the survey line and from deeper depths; hence, there is less confidence in the resistivity values along the edges of the profiles and at deeper depths. Moreover, the inverted resistivity values should be considered spatial averages and not absolute values. Day-Lewis and others (2006) used synthetic CRP tomography models to demonstrate the limitations of CRP for measuring the resistivity of a freshwater target. Because of electrical channeling around the resistive unit and damping of the resistivity values within the inversion, the resistivity of the freshwater target is underestimated. Likewise, the resistivity of the bedrock in this investigation is expected to be underestimated, and thus the inverted resistivity values of the bedrock resistivity are lower (more conductive) than the expected absolute values. The initial interpretations of the inverted profiles assumed a bedrock resistivity of 4 ohm-m, but that assumption often produced bedrock surfaces that were deeper than the bedrock interpreted from the CSP profiles. Based on the results of Profile 1 CSP and CRP data and the results of coring, the bedrock surface was interpreted to be at the contour interval between 1.2 and 2.0 ohm-m. Because of variations in the resistivity of the water column, the resistivity of the earth materials, and the depth of the water, the magnitude of the resistivity at the sediment-bedrock interface varies from profile to profile. The resistivity value used to estimate the bedrock was determined for each profile using core information or depth to a seismic reflection interpreted as bedrock. Both contour intervals (4 and 1.5 ohm-m) were identified on the profiles.

Interpretation of CRP Data

Data were inverted from apparent resistivity to resistivity using the RES2DINV program in efforts to identify the subsurface materials and bedrock interface. Inversion methods attempt to determine a subsurface "true" resistivity model that matches the measured apparent resistivity data with certain constraints. For this investigation, a finite-difference model is modified with each iteration in efforts to minimize the differences between the computed data and the observed or measured resistivity.

Processing CRP data includes the following steps:

- Navigation data for the CRP were processed to convert latitude and longitude in WGS 84 to NAD83, State Plane Coordinates for Connecticut, in meters and then converted to feet.
- Depth to the water bottom, collected with the echo sounder, was processed and used for constrained inversions. Corpscon (v. 6.0.1) was used to convert the data from latitude and longitude to State Plane Coordinates (U. S. Army Corps of Engineers, 2004).
- In Marine Log Manager from Advanced Geosciences, Inc., the continuous string of CRP data was synchronized by time to the GPS navigational data. The data locations were plotted in real-world coordinate plots, and straight-line segments of the continuous data were selected for processing. The CRP data were saved by profile and exported for inversion.
- The files were converted from the unprocessed AGI data format (*.stg) format to the *.dat format using a utility called AGI2DRES (VeeAnn Cross, U.S. Geological Survey, written commun., 2005) making them compatible for input into RES2DINV (Loke, 2001).
- The data were plotted in an apparent resistivity pseudo-section and examined to verify that there is nothing unreasonable and there is no excessive "noise" in the pseudo-section. In RES2DINV, adjacent measurement points are averaged to remove noise. In addition, the data points are plotted and bad data points can be removed manually, if necessary.
- The CRP data were inverted multiple ways—with constrained and unconstrained conditions and with robust (absolute) and smooth (least-squares) algorithms using RES2DINV (Loke, 2001). The unconstrained inversion was inspected to ensure good agreement between the inverted resistivity model and the measured apparent resistivity. The inverted models were inspected for artifacts of the inversion process. In the unconstrained inversions, a check is made to verify that the resistivity of the water column looks similar over the profile and to determine if the depth of water changes significantly. These factors may be problematic in a constrained inversion, where the depth to water can vary but the resistivity of the water is fixed.
- In the constrained inversions, the resistivity of the marine water layer was set to 0.3 to 0.5 ohm-m, typical values for saltwater. The value for the water was checked against the resistivity measured in the closest spaced electrodes. In addition, the water-column values were compared against measurements in the harbor at water-quality monitoring stations (*http://www.Savethesound.org/report2001/har-bridge.htm*, last accessed 21 February 2007) where the reported salinity and temperature values converted to an average of 0.3 ohm-m. The constrained inversions are inspected to specifically assure that the inversion did not become unstable and produce artifacts where there are changes in the depth of water.

When possible, the water column was constrained using the depth to water bottom determined with the echo sounder and a uniform estimate of resistivity in the water column. In some cases, where the depth to the water bottom varied greatly, or when the actual resistivity of the water column varied, the inversions did not converge or did not adequately represent the subsurface. Day-Lewis and others (2006) showed that use of poor constraining values for the water column produces erroneous results; hence, use of unconstrained inversions is preferred when accurate measurements of depth and water resistivity are not available or when the water resistivity varies with depth or distance over the profile. In cases where the resistivity of the water column was not uniform or where the depth of the water column varied, the profile lengths were shortened to include only the areas over the proposed CAD cell, omitting the sections in deeper water. When the constrained inversions for the shortened profiles did not produce reasonable results, the profiles were inverted without constraining the water column and allowing the computed resistivity of the water column to vary. The results were compared and inspected for anomalies in the inversion, and inversion parameters were adjusted until a final reasonable solution was reached. The final inversions were saved, and the best inversion model was chosen for each profile.

The line of interpreted bedrock was drawn on the image of the final inversion, and the depth to reflector was manually digitized, giving a depth to bedrock for every point along the profile, as requested by the USACE. The depths to water bottom and bedrock were measured and shown in a separate plot below the inverted profile, and the results were provided to the USACE in tables and plots relative to MLLW. The results were then compared to the interpreted depth to bedrock for the seismic reflection profiles.

In Bridgeport Harbor, the depth to the water bottom varied across the profiles, and the resistivity of the water column appeared to vary in the unconstrained inversions. For selected profiles, the inverted sections were limited to the zones of interest and to places where the depth to the water bottom was fairly constant. Results of constrained and unconstrained inversions were compared for these shortened profiles.

Geomagnetic Surveying

Geomagnetic methods are used to measure the intensity of the earth's magnetic field (Zohdy and others, 1974; Breiner, 1999). Magnetic anomalies are distortions of the magnetic field relative to the typical direction and intensity of the magnetic field.

Theory of Geomagnetic Surveying

The magnetic signature of any subsurface feature in a geomagnetic survey is dependent on the earth's magnetic field; the size, geometry, orientation, and distance of the source material from the magnetometer; and the magnetic susceptibility of the object. Near-surface magnetic surveys measure the intensity and (or) gradient of the magnetic field. Generally, changes in the magnetic field are caused by lithologic changes in the subsurface, anthropogenic objects that have magnetic properties, and diurnal fluctuations. Igneous and metamorphic rocks, and to a lesser extent sedimentary rocks, have magnetic signatures caused by magnetic minerals, such as magnetite and pyrrhotite. In the continental United States, the magnetic field ranges from 49,000 to 60,000 nT (Zohdy and others, 1974). Examples of anthropogenic objects that can be detected by a magnetometer include metal drums, pipes, cables, boat parts, tools, chains, and other metal debris on or near the bottom of the harbor. Depending on the size of and distance to these targets, the response varies. Breiner (1999) provides a detailed list of examples, including the expected responses from a 15-cm screwdriver at a depth of 4 to 30 m and the expected responses from an automobile over the same range of depths. For this investigation, the magnetic data were used in conjunction with the CRP profiles to help evaluate possible anthropogenic anomalies that might adversely affect the CRP data. In addition, identification of these anomalies may show important targets to avoid during dredging operations.

Equipment and Methods of Magnetometer Data Collection

An optically pumped cesium magnetometer (Smith, 1997) was used in this survey. This instrument makes use of the fact that an electron, such as the lone electron in the outer shell of the cesium atom, has an electric charge and spin, and consequently has a magnetic moment. Furthermore, the energy of the electron varies according to the direction of its spin axis relative to the ambient magnetic field. Measurements of changes in the energy due to changes in orientation of the electrons can be used to calculate the intensity of the ambient magnetic field. The equipment consists of a probe with a glass cylinder (or absorption cell) filled with cesium gas, a cesium-source lamp, a polarizer, and a photocell. A light from a cesium-source lamp is passed through the cesium-vapor-filled bulb, is polarized, and a photocell measures the counts of light passing through the bulb with a frequency-specific counter called a Larmor counter. The frequency content of the signal that passes through the cell is directly proportional to the magnetic field. Although a standard proton precession magnetometer can measure absolute magnetic values, the optically pumped cesium magnetometer can measure to 1 or 2 nT, which is sufficient for most survey applications. The advantage of the cesium magnetometer is that it can collect five times as many readings as the proton-precession meter and still meet most survey objectives.

A marine cesium magnetometer model G882, produced by Geometrics, was used for this investigation. The "fish" was towed at a fixed depth of 7 m below the water surface for

Profiles 1, 2, 4, and 5 and at a depth of 2.5 m for Profiles 3, A, and B. The data were acquired using Geometrics' MagNT acquisition software, at a data collection rate of 10 times per second.

Limitations of Magnetometer Methods

The magnetometer tool ideally is towed at a constant distance above the material being tested. In this investigation, the towing depth was constant but the depths to the water bottom were variable, thus, the height of the instrument above the water bottom varied. The expected effect of the changing depth to water bottom is that as the distance between the magnetometer and a magnetic source increases, the strength of the magnetic field decreases (Breiner, 1999). Larger contrasts in the magnetic strength and larger sources of magnetic materials would be expected to produce larger anomalies. In addition, data quality can be affected by diurnal and temporal variations; these factors are thought to be minimized, however, because the measurements were taken over a short period of time and minimal geomagnetic storms were reported over that time (U.S. Department of Commerce, NOAA, Space Environment Center, *http://Spaceweather.com/* last accessed 31 May, 2006).

Interpretation of Magnetometer Data

The data were processed, displayed, and exported into ASCII files using MagMap, which is produced by Geometrics. In this study, sharp increases or decreases in the magnetic field were considered to be anomalies. Although the interpretation software allows for an accurate modeling of the size, mass, and depth of the anomaly, this interpretation would require additional information such as the exact depth of the water column. For this investigation, only changes in the total field were noted.

Results of Marine Geophysical Surveys

CSP, CRP, and magnetometer data were collected along seven profiles in Bridgeport Harbor during April 2006. Profiles 1, 2, 3, A, and B were located over the proposed southwestern CAD cell, and Profiles 4 and 5 were located over the northern CAD cell (fig. 1). A secondary pilot investigation was conducted in October 2006, to evaluate different seismic sources. This survey was conducted on Profiles D, E, and F over a third proposed CAD cell on the southeastern side of the harbor.

Profile 1

Profile 1 runs southwest to northeast and shows the subsurface beneath the proposed southwestern CAD cell and the navigation channel (fig. 1). The CSP record for Profile 1 in meters below the antenna, which was 1 m below the ambient water surface, is shown in figure 5A. The water level at the time of the survey was 0.5 m above the MLLW datum (table 1). The red line above the CSP plot indicates the extent of the proposed CAD cell. The entire length of Profile 1 with the depth converted from traveltime to depth below MLLW using a velocity of 1,534 m/s and a correction to MLLW level, is shown in figure 5B. The intersections of Profiles A, 3, B, and 2 and the locations of borings FB-06-1, FP-03-04, FP-03-10, and FP-03-13 are shown. In September 2006, FB-06-1 was cored at the intersection of Profile 3 and Profile 1.

Much of the middle section of CSP Profile 1 was adversely affected by water-bottom multiples that obscured the subsurface. The water bottom and the multiples were clear and continuous in the data record. The reflection of the bedrock surface, however, was discontinuous and difficult to trace across the profile. At a distance of about 900 m from the southwestern end of the profile, a discontinuous reflector was observed at a depth of 37.2 m below MLLW. The interpretation of this reflector as bedrock has a good correlation with the depth to refusal of 37.5 m below MLLW observed in borehole FP-03-10. The reflector appears to be irregular with low amplitude and low frequency. A more continuous reflector was identified from about 10 to 350 m along the profile. The appearance of this reflector is similar to the one observed at about 900 m along the profile, and was thus interpreted as bedrock. This reflector varies in depth from 4 to 14 m below MLLW.

At the intersection of Profile 1 with Profile A, this seismic record shows a reflector at 4.4 m below MLLW. On the seismic record for Profile A, the bedrock was interpreted at 2 m below MLLW, but sloped downwards north of the intersection. At the intersection of CSP Profiles 1 and 3, the Profile 1 record shows a bedrock reflector at 10 m below the MLLW. On Profile 3, there were no reflection data at the exact intersection with Profile 1, but at the closest reflector about 27 m away on Profile 3, the depth to the bedrock reflector was 8.8 m below MLLW. Boring FB-06-1 was drilled in September 2006 at the intersection of the CSP Profiles 1 and 3 and magnetometer Profile 3. In the boring, there was 11 m of sediments. The boring log indicated 3 m of sand, overlying 6 m of silty sand, above 2 m of coarse sand and weathered bedrock, with fractured schist at a depth of about 12.5 m below MLLW. These results suggest that there is fairly good correlation between Profile 1 and the boring and marginal to fair agreement with Profile 3. Consequently, the data quality was considered to be of fair quality for almost the entire profile. The correlation of the reflector with boring data increases the confidence in the interpretation of these reflectors as bedrock. At the intersections of Profile 1 with Profiles B and 2, no reflections were observed because of the multiples and the poor signal penetration into the subsurface. In general, the reflectors seen in Profile 1 are fair to good quality.

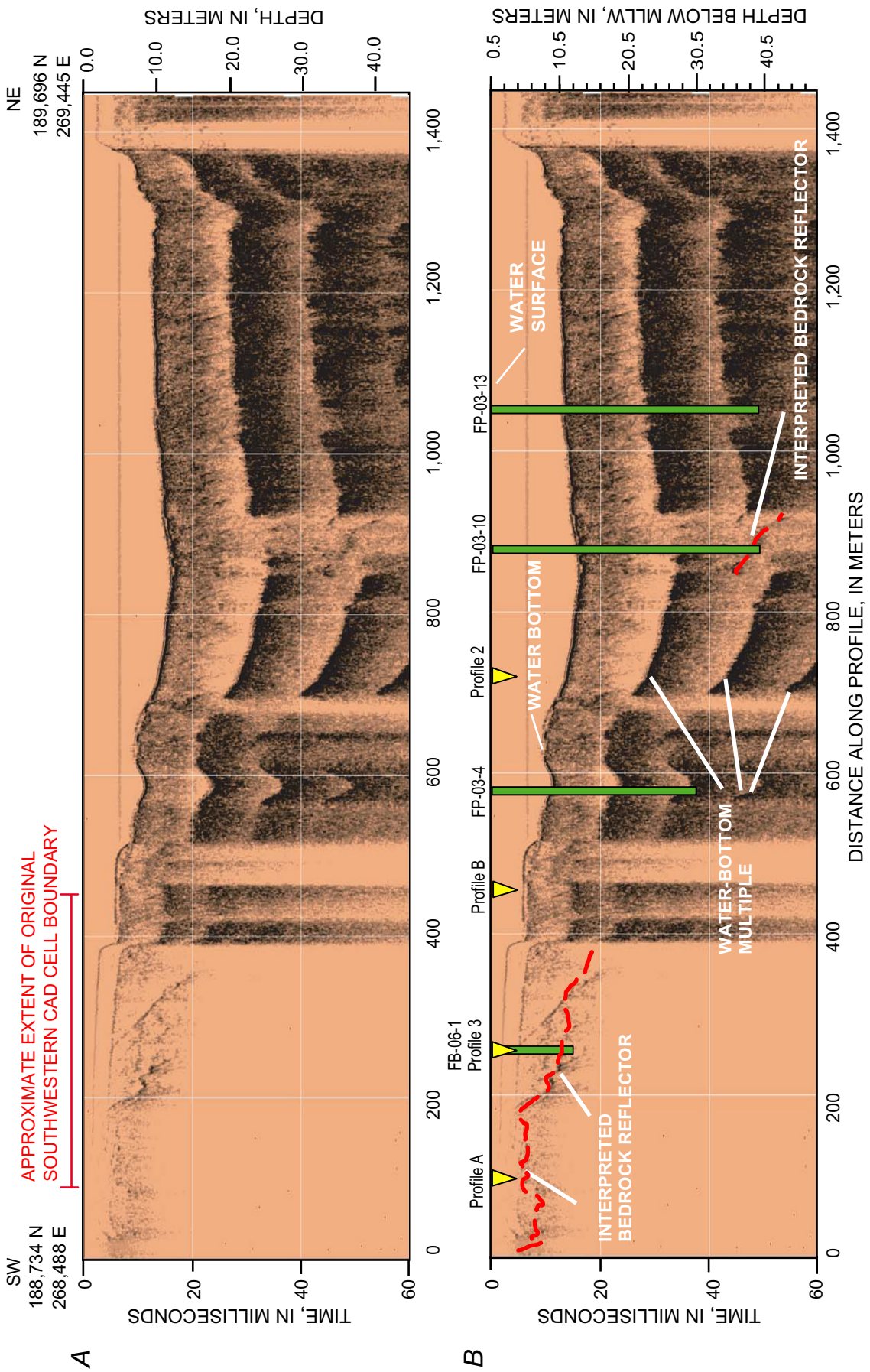

Figure 5. Swept-frequency seismic section from Profile 1, Bridgeport Harbor, Bridgeport, Connecticut, showing (*A*) the unprocessed data and (*B*) the interpretation. Velocity of sound in salt-saturated sediments of 1,534 meters per second was used to estimate depth. Depths in (*A*) are shown in meters (m) below antenna, which was 1 m below the water surface. At the time of data collection, the water surface was 0.5 m above mean low-low water level (MLLW). Depths in (*B*) are below MLLW. End-point positions are in Connecticut State Plane Coordinate System using the North American Datum of 1983, in meters. Green markers identify locations of borings shown to refusal, and yellow markers indicate location of intersections with other survey lines. The red dashed line is the interpreted bedrock surface.

The CRP data for Profile 1 were collected nearly parallel to the CSP profile, but were offset by as much as 50 m on the southwestern end of the profile (fig. 1). The resistivity data and interpretation are shown in figure 6. The shallow resistive zones on the southwestern side of the profile 0–400 m is consistent with the interpretation of resistive bedrock under the more conductive sediments. The initial interpretation of bedrock along this profile yielded depths to bedrock of 20 m where the CSP profile indicated it was 10 m to bedrock. One possibility for this discrepancy is the offset in the profiles. Another possibility is that the initial interpretation of CRP data for Profile 1 used the 4-ohm-m contour interval as the estimate of the bedrock surface, which proved to be too deep when compared to the boring data. It appears from figure 6A that a resistivity contour between 1.2 to 2.0 ohm-m might be a better estimate of the bedrock surface. Over the middle of the profile and the northeastern sections of the profile, the water was too deep to image the bedrock, so comparisons were only done on the southwestern side over the CAD cell area.

Magnetometer data were collected for Profile 1, but the data were corrupted, so no magnetometer data are plotted for Profile 1.

Profile 2

Profile 2 runs west to east through the southwestern CAD cell (fig. 1). The CSP record for Profile 2 in meters below the antenna, which was 1 m below the ambient water surface (table 1), is shown in figure 7A. The water level at the time of the survey was 0.5 m above the MLLW datum (table 1). The red line above the CSP plot indicates the original extent of the proposed southwestern CAD cell. The proposed CAD cell extends approximately 140 m west of the completed CSP profile. The entire length of Profile 2 with the depth converted from traveltime to distance using a velocity of 1,534 m/s and a correction to MLLW level, is shown in figure 7B. This profile passes near borings FP-03-09 and FP-03-11, which were drilled through sediments to more than 30 m below MLLW. The intersections of Profile 2 with Profiles 3, B, and 1 also are shown on the plot. The western end of CSP Profile 2 as delineated by the USACE was inaccessible at the time of the survey, because the depth of water was less than 1 m at the time of data collection.

Most of this seismic profile was adversely affected by multiple reflections off of the hard water bottom or by gas entrapped in the sediments. Bedrock reflections were only observed over a short segment of the profile, 0 to 42 m from the western end of the profile. Profile 2 crosses Profile 3 about 21.3 m from the western end of the profile, where there is a bedrock reflector interpreted at a depth of 5.4 m below MLLW. At the same intersection point on Profile 3, the bedrock reflector was interpreted at a depth of 6.2 m below MLLW. Profile 2 crosses Profiles B and 1, but no bedrock reflections could be determined in Profile 2 at these locations. Two borings, FP-03-09 and FP-03-11, were drilled near Profile 2. Both had depths to bedrock that were greater than 30 m, but no reflections were seen at these locations. Because of the poor signal penetration, the data quality rating for this profile was very poor.

The CRP data for Profile 2 were collected nearly parallel to the CSP profile, but offset a little on the southwestern end of the profile (fig. 1). The depth of water is shallower over the CAD cell than over the rest of the profile towards the east. In the constrained inversion for the entire profile, the resistivity showed an abrupt change where the depth of water increased from shallow to deep, indicating a possible artifact of the geometry in the inversion. Because the zone of interest is over the area of the proposed CAD cell, the data from that part of the profile were inverted separately (fig. 8). In this shortened profile, the resistivity increased and bedrock was interpreted at a depth of about 8 to 15 m below the MLLW, coincident with the resistivity contour between 1.2 to 2.0 ohm-m. The water temperature has its highest value of 11.5°C at about 300 m from the western end of the profile, just outside the eastern edge of the proposed southwestern CAD cell boundary. This temperature spike appears to coincide with a change in the depth of the water column and is associated with an increase in resistivity. The temperature and increased resistivity may indicate possible ground-water discharge or may be an artifact of the inversion, compensating for a large change in the depth of the water column.

The magnetometer data for Profile 2 show a fairly uniform distribution with magnetic field values around 53,100 nT under the CAD cell. The strength of the magnetic field appears to drop slightly where the depth of the channel increases. There also may be small anomalies at 10, 160, 320, 460, and 825 m from the western end of the profile (fig. 9).

Profile 3

Profile 3 runs north to south, parallel to the shore, along the long axis of the proposed southwestern CAD cell. The navigation data for this profile were corrupted; hence, the end points of the profile were used and points along the line were evenly incremented. The CSP record for Profile 3 in meters below the antenna, which was 1 m below the ambient water surface, is shown in figure 10A. At the time of data acquisition the MLLW correction was 1 m for CSP and 0.3 m for CRP (table 1). The red line above the CSP plot indicates the extent of the proposed CAD cell. The entire length of Profile 3 with the depth converted from traveltime to depth below MLLW using a velocity of 1,534 m/s and a correction to MLLW level is shown in figure 10B. The locations of intersections with Profiles 2 and 1, and borings FP-03-03 and FP-06-1 also are shown.

In general, the water bottom and multiples are the strongest and most continuous reflectors in the CSP record. Over the middle to southern part of the record, there is relief along the interpreted bedrock surface that does not mimic the water bottom and clearly can be distinguished from the

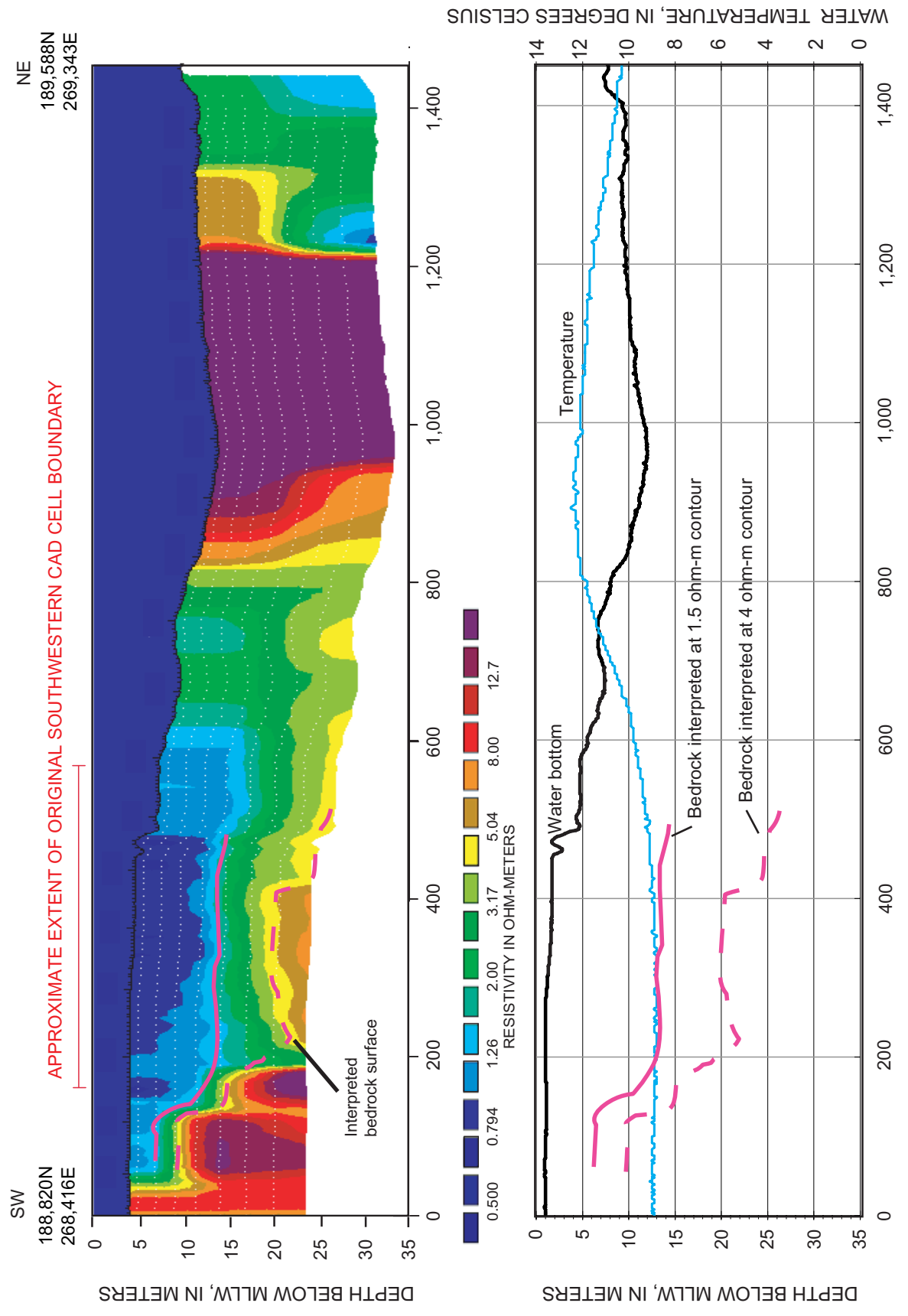

Figure 6. Continuous resistivity survey from Profile 1, Bridgeport Harbor, Bridgeport, Connecticut, showing (*A*) the inverted, constrained data, and (*B*) the interpretation of depth to bedrock, measured depth to water bottom, and temperature of near-surface water in degrees Celsius. The solid and dashed red lines show the interpreted bedrock surface. Depths are shown in meters below the mean low-low water (MLLW) surface. Profile runs southwest to northeast. End-point positions are in Connecticut State Plane Coordinate System using the North American Datum of 1983, in meters.

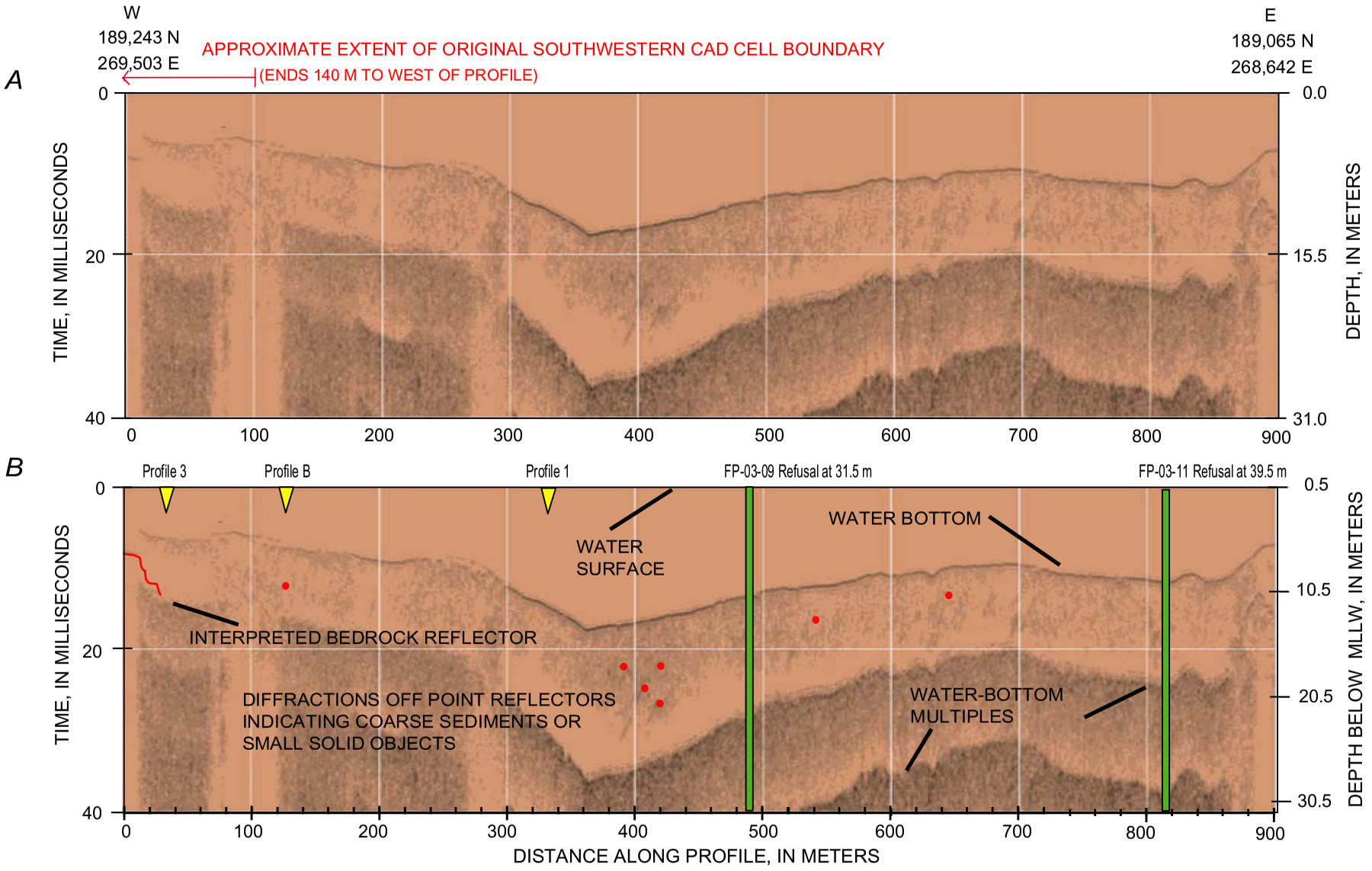

Figure 7. Swept-frequency seismic section from Profile 2, Bridgeport Harbor, Bridgeport, Connecticut, showing (*A*) the unprocessed data and *(B*) the interpretation. Velocity of sound in salt-saturated sediments of 1,534 meters per second was used to estimate depth. Depths in (*A*) are shown in meters (m) below antenna, which was 1 m below the water surface. At the time of data collection, the water surface was 0.5 m above mean low-low water (MLLW) level. Depths in (*B*) are below MLLW. End-point positions are in Connecticut State Plane Coordinate System using the North American Datum of 1983, in meters. Green markers identify locations of borings shown to refusal, and yellow markers indicate location of intersections with other survey lines. The red dashed line is the interpreted bedrock surface.

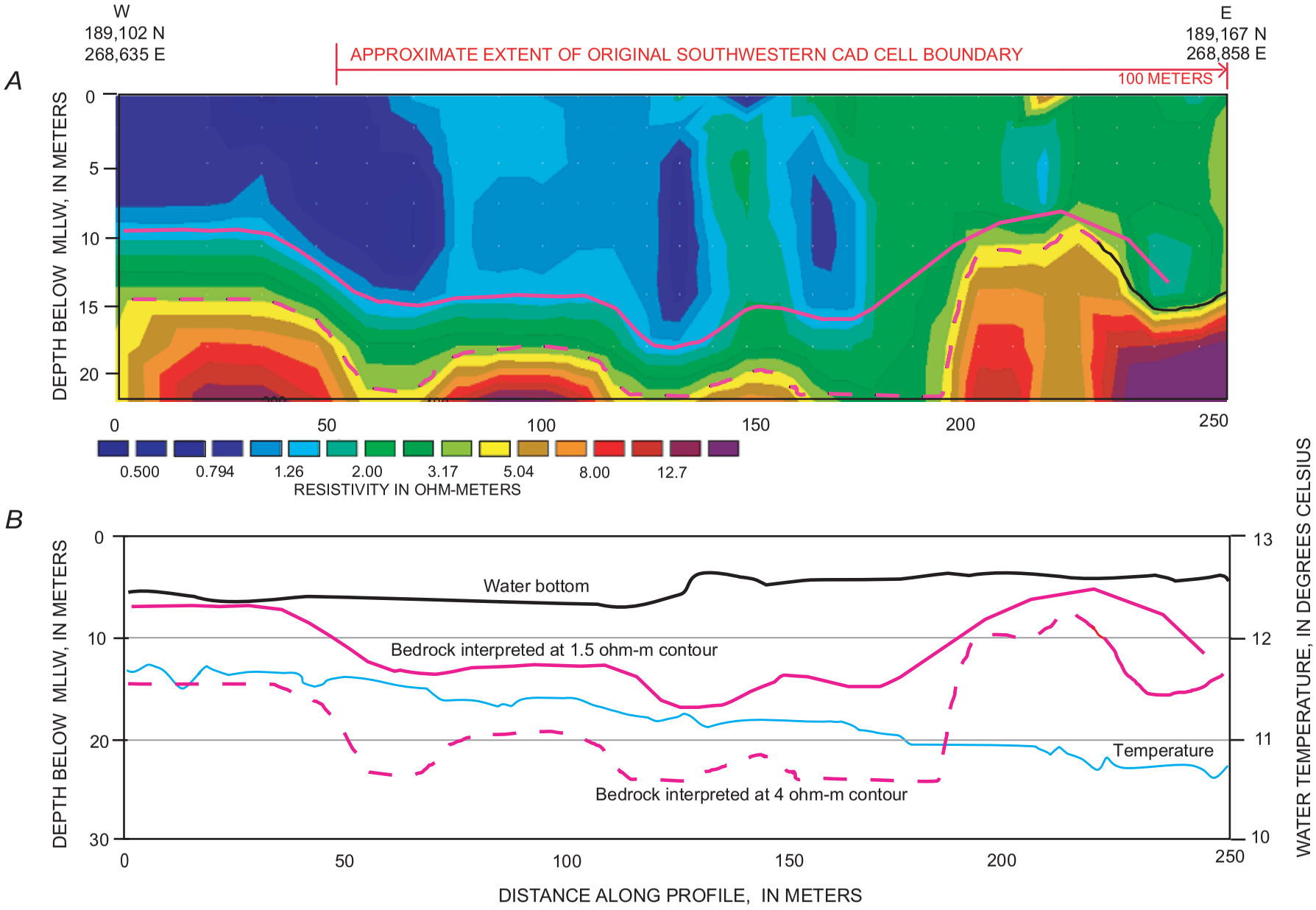

Figure 8. Continuous resistivity survey from western end of Profile 2, Bridgeport Harbor, Bridgeport, Connecticut, showing (*A*) the unconstrained, robust inversion, and (*B*) the interpretation of depth to bedrock, measured depth to water bottom, and temperature of near-surface water in degrees Celsius. Depths are shown in meters below the mean low-low water (MLLW). The original southwestern CAD cell extends about 100 meters to the east of the profile. End-point positions are in Connecticut State Plane Coordinate System using the North American Datum of 1983, in meters.

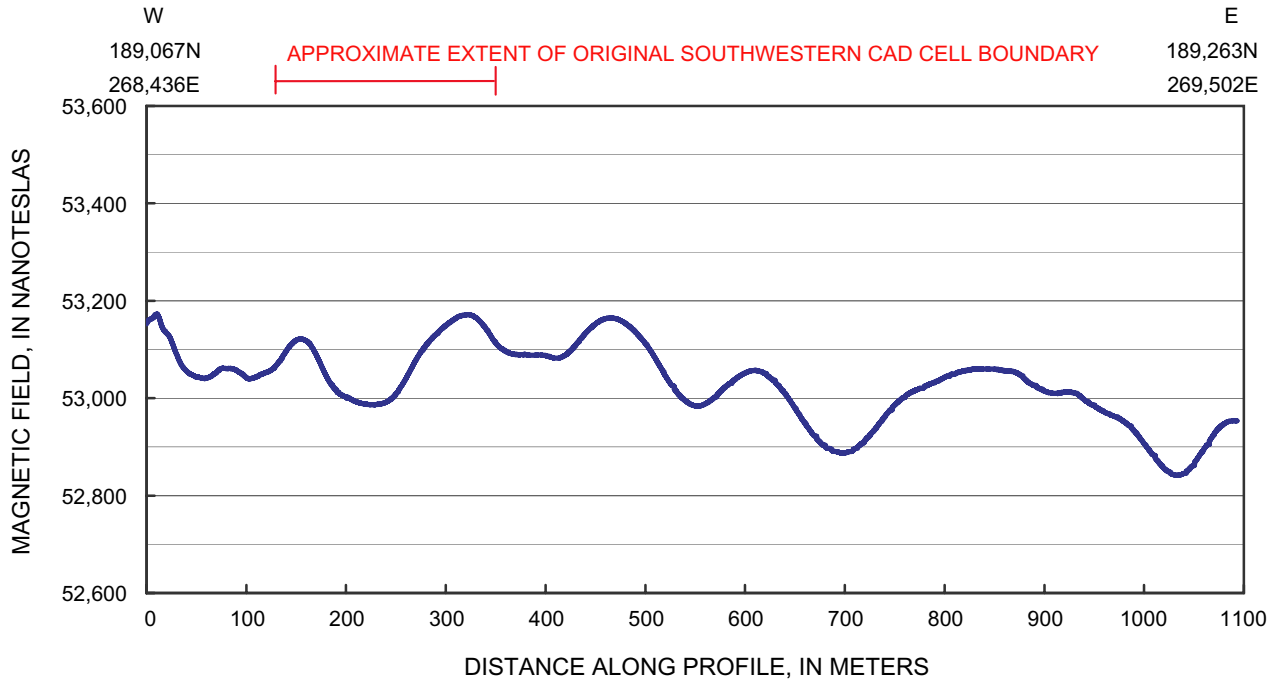

Figure 9. Magnetometer data collected along Profile 2, Bridgeport Harbor, Bridgeport, Connecticut. End-point positions are in Connecticut State Plane Coordinate System using the North American Datum of 1983, in meters.

multiples. Elsewhere in the record, it is difficult to distinguish the bedrock surface from the multiples. At the intersection of Profiles 3 and 2, there are no interpreted reflectors. At the intersection of Profiles 3 and 1, the interpreted depth to bedrock in Profile 3 is 6.2 m below MLLW, and the interpreted depth to bedrock in Profile 1 is 10 m below MLLW. This intersection is coincident with boring FB-06-1, where there were 11 m of unconsolidated materials and bedrock determined at a depth of 12.4 m below MLLW. However, there is a reflector on Profile 3 within 30 m of the intersection of Profiles 3 and 1 that shows the bedrock at 8.8 m below MLLW. These results suggest that there is fairly good correlation between Profile 1 and the boring and marginal to fair agreement between Profiles 1 and 3. Consequently, the data quality rating for Profile 3 was considered to be fair for almost the entire profile.

Profile 3 CRP data were inverted using a robust, unconstrained inversion (fig. 11A). A resistivity of 4 ohm-m initially was used to estimate the bedrock surface (dashed line). For most of the profile from 100 to 400 m, the data show a depth to water bottom of 1 to 5 m and interpreted depth to bedrock of 7 to 9 m; on the northern end of the profile where the depth to the water was deepest, the data show a depth to water bottom of 10 to 16 m. Assuming a resistivity of 1.2 to 1.5 ohm-m, the interpreted depth to bedrock was about 5 to 7 m over most of the profile (fig. 11A, solid line). The gap in the resistivity profile from 70–90 m is an artifact in the data; hence it was ignored in the interpretation of the bedrock surface. Where the CRP and CSP surveys for Profile 3 cross, at about 185 m from the northern end of CRP profile (fig. 11), interpreted depth to bedrock in the CRP was 7.3 m below MLLW using the initial estimate for the bedrock interface at 4 ohm-m and was 5.3 m below MLLW using the lower resistivity interpretation of the bedrock. There were no reflectors interpreted for that part of the seismic record.

The temperature changed gradually over the length of the profile, changing a total of 3°C, centered near the midpoint of the profile shown and near the change in the depth to the water bottom (fig. 11B). The temperature was lowest over the southern, more shallow part of the profile. The cause of the change in temperature is unknown.

The magnetometer data show a steep decline in the strength of the magnetic field about 330 m from the northern end of the line, in about the middle of the profile (fig. 12). On the northern end of the profile, the magnetic field was about 53,000 nT. At nearly 200 m along the line, the magnetic field increases to greater than 53,300 nT and remains high to about 330 m along the profile. At 380 m along Profile 3, the magnetic field declines to about 52,630 nT, and then it gradually climbs back to a level of 53,100 nT at 680 m. The location of this magnetic anomaly, which is characterized by an increased spike and sharp decline, is approximately in the middle of the proposed CAD cell (fig. 12), and is similar in magnitude, location, and shape to the anomaly in adjacent Profile A. Because of the magnitude and possible continuity of this anomaly with that in the adjacent line, this magnetic anomaly may indicate a large-scale anthropogenic feature, such as a pipeline.

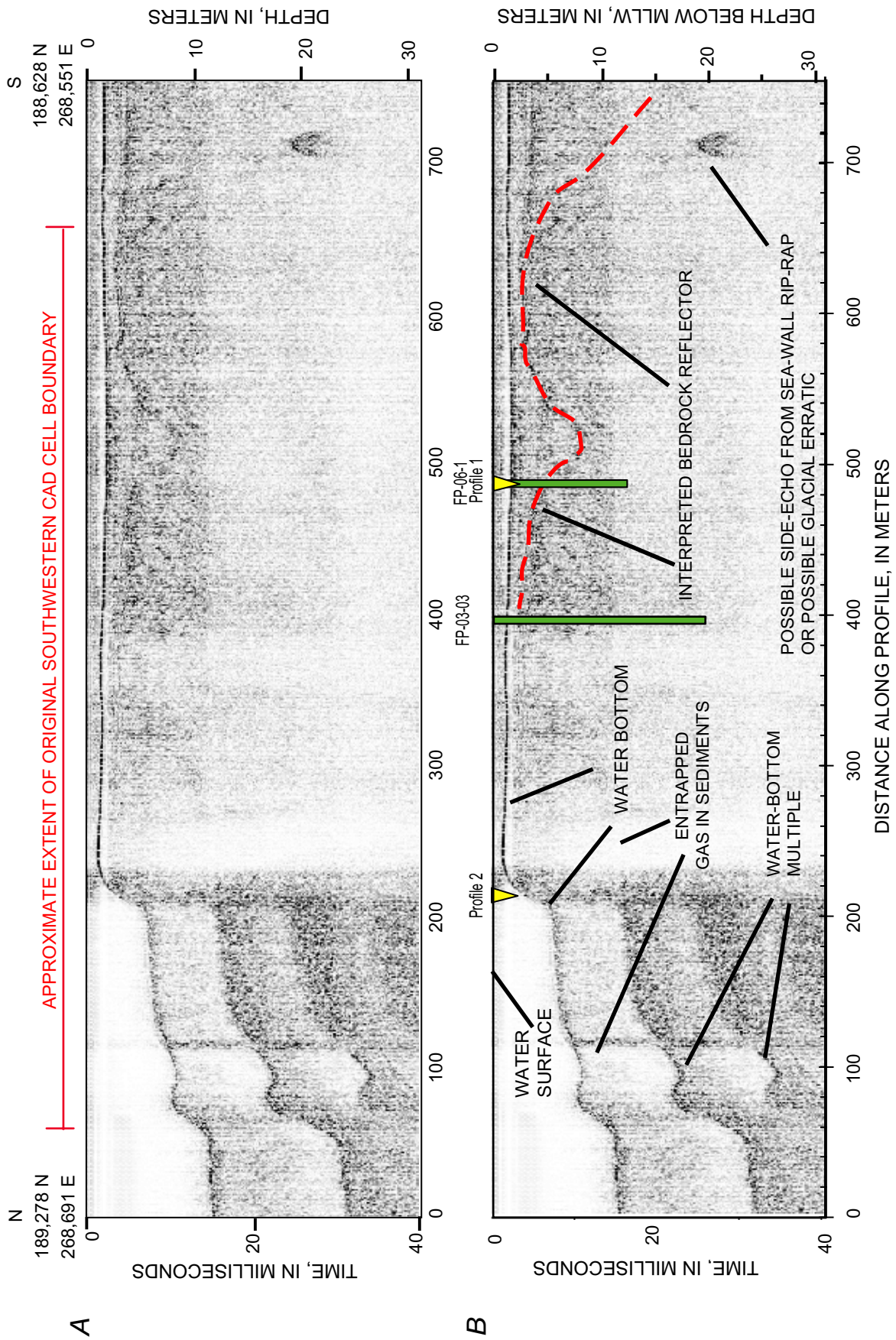

Figure 10. Swept-frequency seismic section from Profile 3, Bridgeport Harbor, Bridgeport, Connecticut, showing (*A*) the unprocessed data and (*B*) the interpretation. Velocity of sound in salt-saturated sediments of 1,534 meters per second was used to estimate depth. Depths in (*A*) are shown in meters (m) below antenna, which was 1 m below the water surface. At the time of data collection, the water surface was 1.0 m above mean low-low water level (MLLW). Depths in (*B*) are below MLLW. End-point positions are in Connecticut State Plane Coordinate System using the North American Datum of 1983, in meters. Green markers identify locations of borings shown to refusal, and yellow markers indicate location of intersections with other survey lines. The red dashed line is the interpreted bedrock surface.

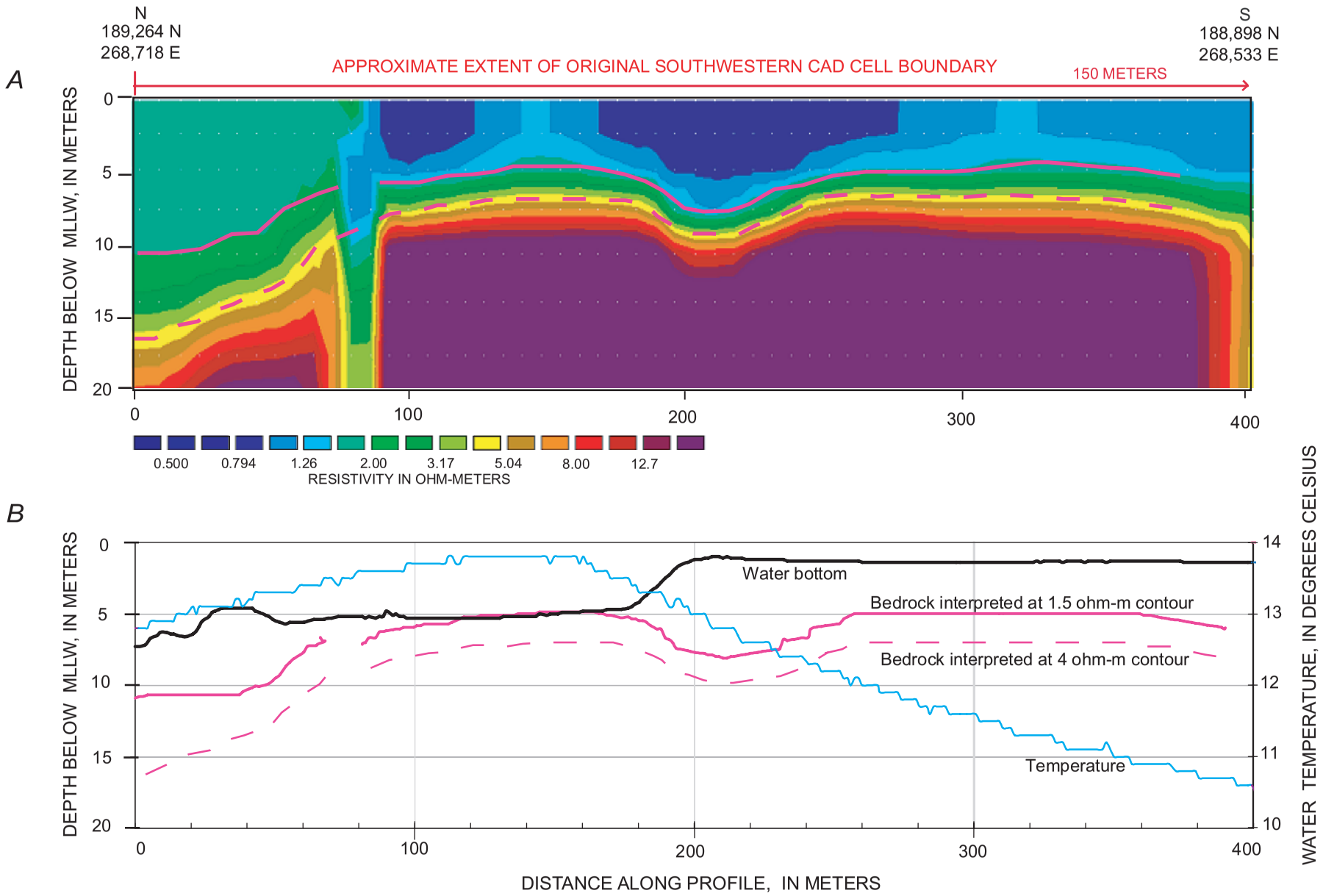

Figure 11. Continuous resistivity survey from Profile 3 over the CAD cell, Bridgeport Harbor, Bridgeport, Connecticut, showing (*A*) the unconstrained, robust inversion, and (*B*) the interpretation of depth to bedrock, measured depth to water bottom, and temperature of near-surface water in degrees Celsius. Depths are shown in meters below the mean low-low water (MLLW). End-point positions are in Connecticut State Plane Coordinate System using the North American Datum of 1983, in meters.

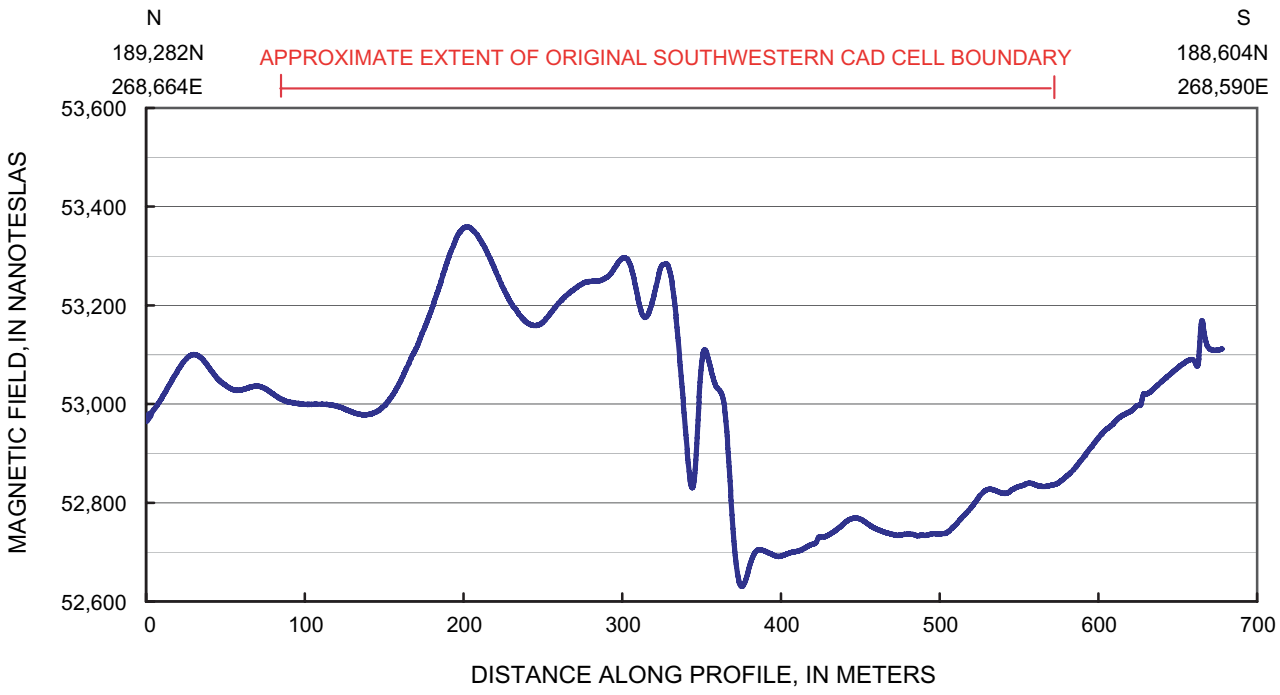

Figure 12. Magnetometer data collected along Profile 3, Bridgeport Harbor, Bridgeport, Connecticut. End-point positions are in Connecticut State Plane Coordinate System using the North American Datum of 1983, in meters.

Profile A

Profile A runs north to south and parallels the long axis of the proposed southwestern CAD cell. The CSP record for Profile A in meters below the antenna, which was 1 m below the ambient water surface, is shown in figure 13A. The red line indicates the extent of the proposed southwestern CAD cell along Profile A. At the time of CRP and CSP collection, the MLLW correction was 0.27 m (table 1). The entire length of Profile A with the depth converted from traveltime to depth below MLLW using a velocity of 1,534 m/s and a correction to MLLW level is shown in figure 13B.

The water bottom and multiple reflections produced as a result of gas-filled sediments or a hard water bottom were clear, strong, and continuous in the seismic record. The reflection of the bedrock surface appears to be continuous and traced in the seismic record above, below, and through the multiples. From about 70 to 300 m along the profile, the bedrock approximately parallels a water-bottom multiple. Small variations in topography along the reflector interpreted as bedrock surface distinguish it from the water-bottom multiple. This indicates that the water bottom is nearly parallel to the bedrock surface over this part of the profile. Over the southern part of the profile, the bedrock surface rises and declines. From about 300 to 420 m along the profile, the bedrock surface declines to a depth of about 5 m below MLLW; from 420 to 490 m the bedrock surface rises to about 2 m below MLLW; and from there to the end of the profile, it declines to about 3.7 m below MLLW. The undulating bedrock surface on the southern half of the profile clearly differs from the water-bottom multiple. Repeat interpretations of the bedrock reflectors show good redundancy, thus improving confidence in the interpretation. The data quality rating for this profile was considered to be fair.

At the intersection of Profiles A and 1, the seismic record for Profile 1 indicates the bedrock is 4.5 m below MLLW. For the same intersection, this seismic record for Profile A shows a reflector at 3.7 m below MLLW. The projected intersection of Profiles A and 2 also is shown on the Profile A; however, no data are available for comparison at this point, because the southwestern end of Profile 2 could not be collected because of shallow water conditions when Profile 2 was surveyed. In general, Profile A shows bedrock reflectors that are shallower than the reflections observed in Profiles 3 and B, which is consistent with the bedrock surface climbing upwards toward the land surface on shore to the west. Diffractions and chaotic reflections in the upper part of the seismic record suggest the sediments are coarse rather than fine. Above the reflector interpreted as the top of bedrock, there are several small-scale, discontinuous features that appear to be linear and may represent layering in the sediments. In addition, there is a strong, steeply dipping reflection that extends below the reflection interpreted as the top of bedrock. This reflection may represent a fracture zone within the bedrock.

CRP for Profile A was run concurrently along the same line as the CSP survey (fig. 1). The CRP data were interpreted with an unconstrained inversion, and the bedrock surface was selected as the 4-ohm-m resistivity contour (fig. 14A). The interpreted depth to bedrock surface has a similar topography as the seismic profile, but the depth is considerably deeper

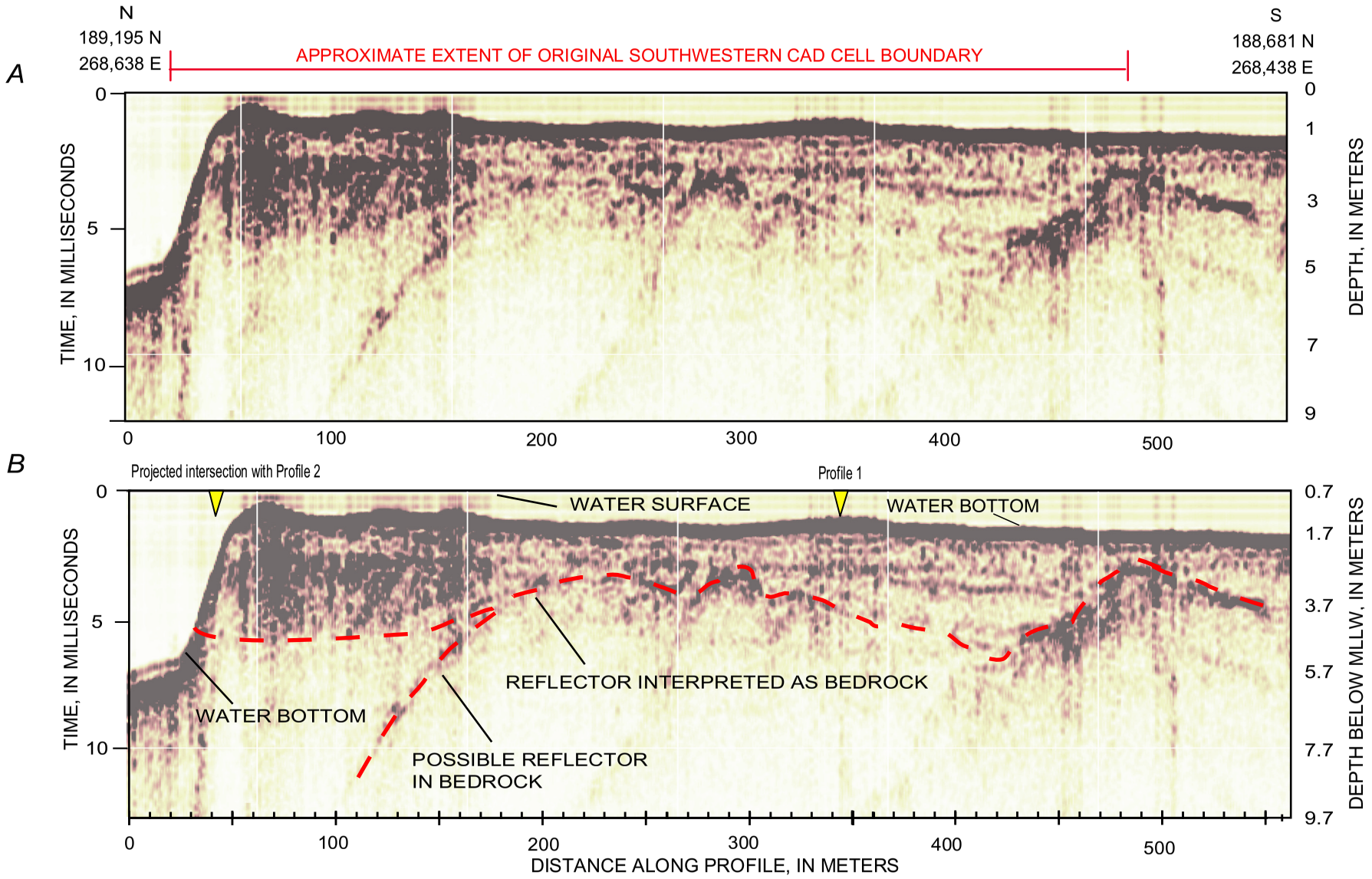

Figure 13. Swept-frequency seismic section from Profile A, Bridgeport Harbor, Bridgeport, Connecticut, showing (*A*) the unprocessed data and (*B*) the interpretation. Velocity of sound in salt-saturated sediments of 1,534 meters per second was used to estimate depth. Depths in (*A*) are shown in meters (m) below antenna, which was 1 m below the water surface. At the time of data collection, the water surface was 0.3 m above mean low-low water level (MLLW). Depths in (*B*) are below MLLW. End-point positions are in Connecticut State Plane Coordinate System using the North American Datum of 1983, in meters. Yellow markers indicate location of intersections with other survey lines. The red dashed line is the interpreted bedrock surface.

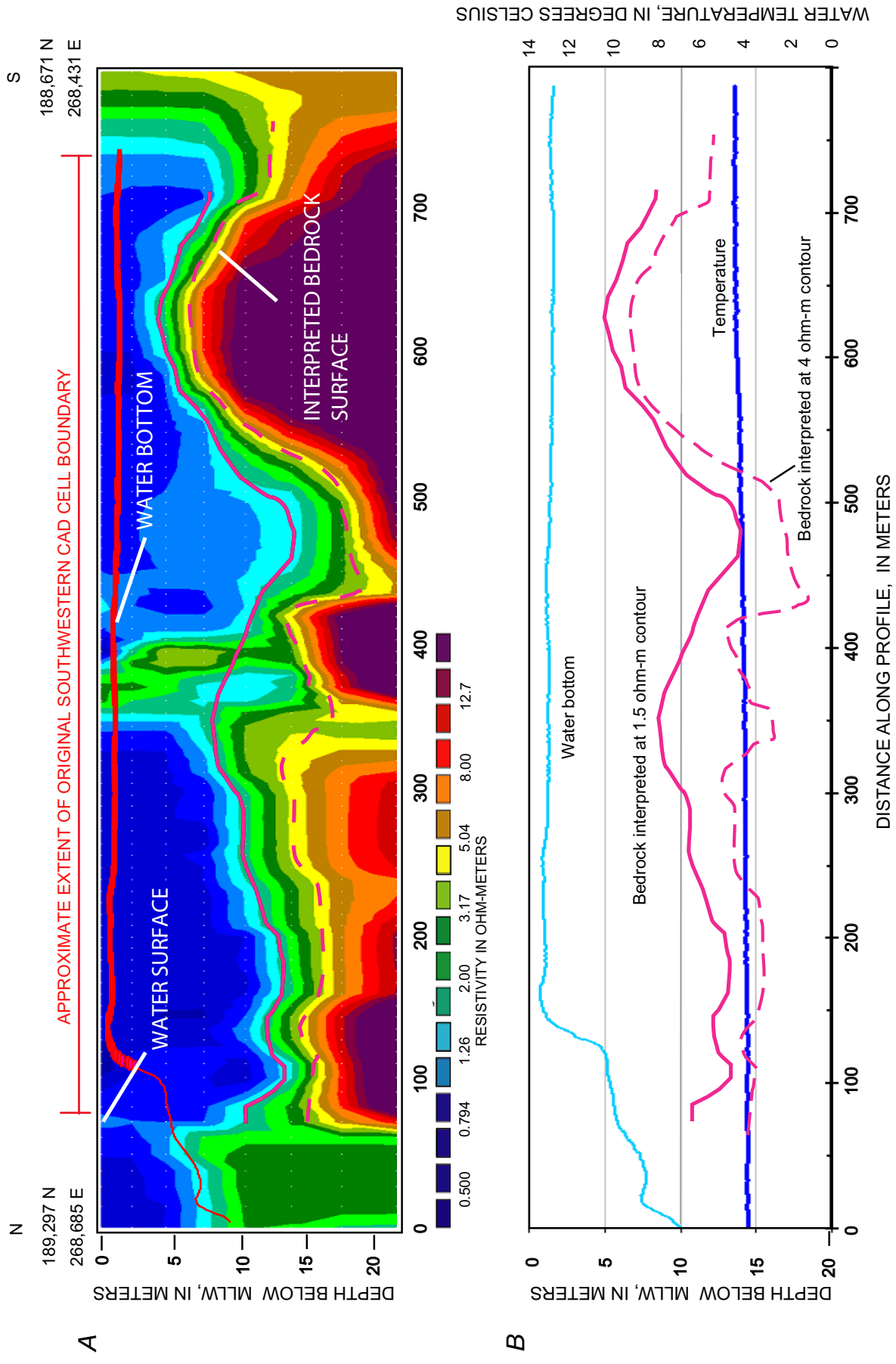

Figure 14. Continuous resistivity survey from Profile A, Bridgeport Harbor, Bridgeport, Connecticut, showing (*A*) the inverted, constrained data, and (*B*) the interpretation of depth to bedrock, measured depth to water bottom, and temperature of near-surface water in degrees Celsius. The solid and dashed red lines show the interpreted bedrock surface. Depths are shown in meters below the mean low-low water (MLLW) surface. The profile runs southwest to northeast. End-point positions are in Connecticut State Plane Coordinate System using the North American Datum of 1983, in meters.

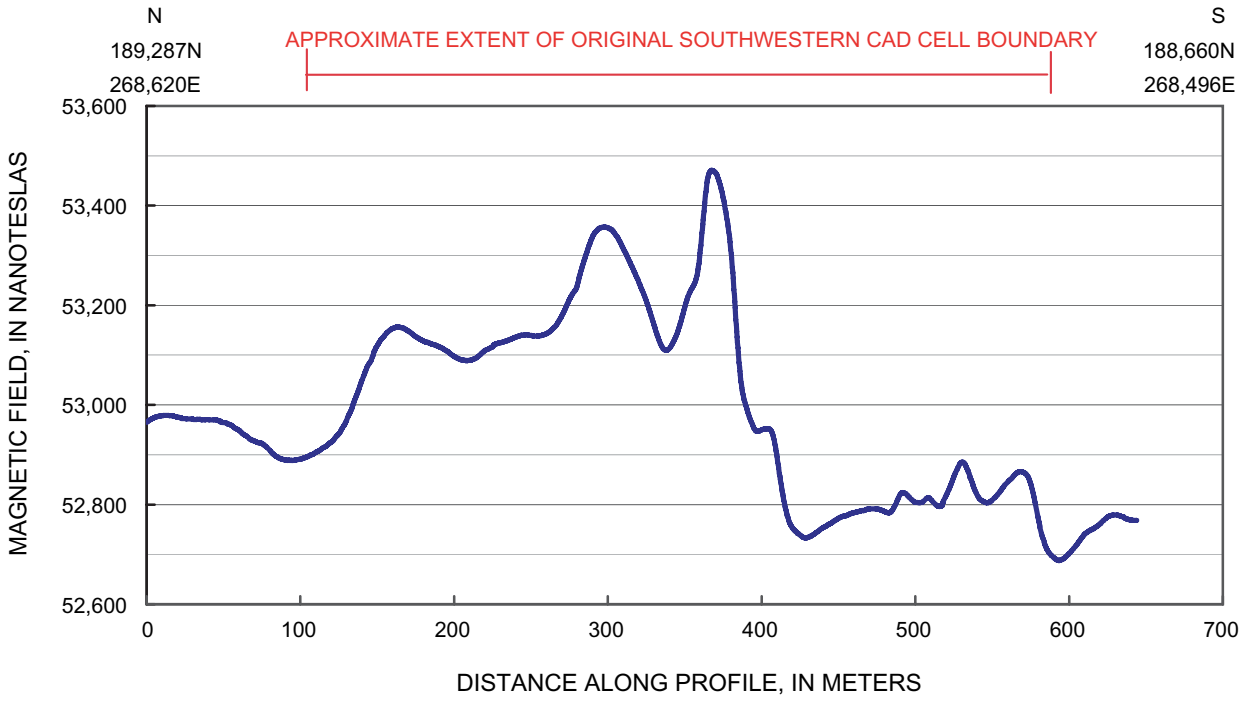

Figure 15. Magnetometer data collected along Profile A, Bridgeport Harbor, Bridgeport, Connecticut. Endpoint positions are in Connecticut State Plane Coordinate System using the North American Datum of 1983, in meters.

than in the CSP, and ranged from 6 m on the southern end of the CRP profile to 15 m on the northern end of the profile (fig. 14B). When the 1.2- to 2.0-ohm-m contour is used, the depth is shifted upwards and ranges from 5 to 12 m, which is still deeper than the interpretation of the CSP for Profile A.

The magnetometer data for Profile A indicate an anomaly near the middle of the proposed CAD cell (fig. 15). There is a positive magnetic spike at about 370 m from the northern end of the line, a sharp decline to 410 m, and low magnetic values to the end of the profile. Other possible minor anomalies occur at 160 and 300 m along the profile. The large anomaly at 350 to 400 m is coincident with the anomaly in the adjacent Profile 3. There is no change in temperature or water-bottom topography coincident with this magnetic anomaly; the CRP data, however, appear to be adversely affected by the zone of increased magnetism that may channel the current away from the surroundings and cause a shallow resistive artifact.

Profile B

Profile B runs north to south and parallels the long axis of the proposed southwestern CAD cell. It roughly parallels Profiles 3 and A and is the furthest east from the shore of these three profiles (fig. 1). The CSP record for Profile B in meters below the antenna, which was 1 m below the ambient water surface, is shown in figure 16A. At the time of data acquisition the MLLW correction for CSP and CRP was 0.2 m (table 1). The red line above the CSP plot indicates the extent of the proposed southwestern CAD cell along Profile B. The entire length of Profile B with the depth converted from traveltime to depth below MLLW using a velocity of 1,534 m/s and a correction to MLLW level is shown in figure 16B. Profile B crosses Profiles 1 and 2. The CSP and CRP profiles were collected concurrently.

At the intersection of Profile B and Profile 2, at 135 m from the northern end of the line, no bedrock reflectors are seen in Profile B. At the intersection of Profiles B and 1, about 265 m from the northern end of the Profile B, Profile B indicates a possible bedrock reflector at 12.8 m below MLLW. For the same intersection, Profile 1 does not show any reflectors at the intersection; however, there was one possible reflector or diffraction at a depth of 12 m below MLLW. The reflector quality was quite poor because any subbottom reflectors were masked by the water-bottom multiple; hence, it was not shown on Profile 1. Boring FP-03-03, which is about 50 m east of the Profile B, at about 400 m from the northern end of the line, showed a depth to refusal of 20 m below MLLW. These boring data may give some validity to the interpreted point reflector observed at a depth of about 18 m at about 420 m from the northern end of the profile.

Regardless of these coincident interpretations, the data quality of Profile B was fairly poor. Because of the strong reflections off the water bottom and multiples of the water bottom, any picks of reflections off the bedrock surface are difficult in this record, and this comparison to Profile 1 makes the interpretation of the reflectors in Profile B more suspect. In addition, there was poor replication in the interpretation of the bedrock surface between redundant interpretations,

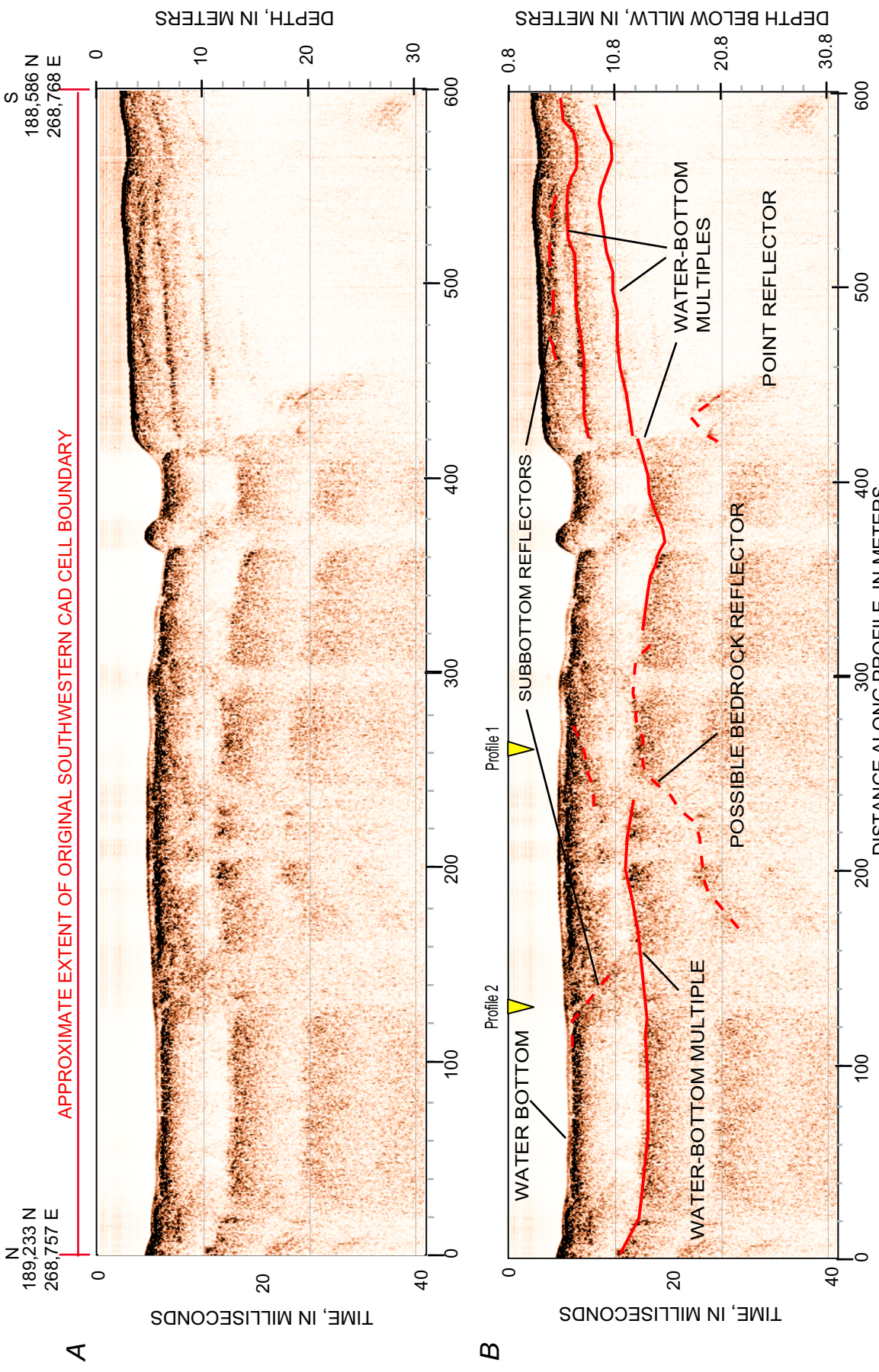

Figure 16. Swept-frequency seismic section from Profile B, Bridgeport Harbor, Bridgeport, Connecticut, showing (*A*) the unprocessed data and (*B*) the interpretation. Velocity of sound in salt-saturated sediments of 1,534 meters per second was used to estimate depth. Depths in (*A*) are shown in meters (m) below antenna, which was 1 m below the water surface. At the time of data collection, the water surface was 0.2 m above mean low-low water level (MLLW). Depths in (*B*) are below MLLW. End-point positions are in Connecticut State Plane Coordinate System using the North American Datum of 1983, in meters. Yellow markers indicate location of intersections with other survey lines. The red dashed line is the interpreted bedrock surface and the solid red line indicates water-bottom multiples.

with one set of interpretations being coincident with a water-bottom multiple. The data quality rating for this CSP profile is considered to be poor.

The CRP record for Profile B is shown in figure 17. The original CRP profile over the proposed southwestern CAD cell had significant topographic changes in the water bottom along the profile. These changes in the depth of the water column manifested as artifacts in the inversion of the complete profile; hence the line was shortened to just the area over the CAD cell where the water depth was about 5 m deep. The high resistivity zone on the northern end of the profile shows more artifacts of the inversion and the associated change in the water depth at 25 to 30 m from the southwestern end of the profile. Boring FP-03-03, which is at about 5 m along the profile (in fig. 17), had a depth to refusal of 20 m below MLLW. This verification point on the northern end of figure 17 supports the interpretation of the northern end of the profile as an artifact of the inversion. Thus, even though the 4-ohm-m contour was used to interpret the depth to bedrock surface, the steep 4-ohm-m contour on the northern end of the line (from 30 to 60 m) was ignored and was not interpreted as bedrock. Over the remaining section of Profile B, the 4-ohm-m contour was 20 to 25 m deep, which is at the functional limit of the CRP equipment. There were no reflectors in the CSP record for this part of the profile for comparison.

The magnetometer data for Profile B is shown from north to south (fig. 18). At the northern end of Profile B, the values are between 53,000 and 53,200 nT, which is similar to the values on northern end of Profiles A and 3. At about 250 m from the northern end of the line, the magnetism starts a decline to about 52,700 nT at about the center of the profile (at 400 m) and in the middle of the proposed southwestern CAD cell. From this magnetic low to the southern end of Profile B, the magnetic values increase to a maximum of 53,570 nT at about 770 m from the northern end of the line. Other possible minor anomalies occur at 80 and 220 m along the profile. The gradual increase in magnetism over the southern half of the profile is similar in character to Profile 3 to the west. There is no apparent change in water-bottom topography coincident with these magnetic anomalies.

CSP Profiles D, E, and F on the Southeastern Side of Bridgeport Harbor

Seismic lines on the southeastern side of the harbor were collected using the 3.5-kHz-tuned transducer and the boomer-plate analog sound sources, and the SB-216s chirp antenna. A grid was established over the proposed southeastern CAD cell, with survey lines going east to west across the entire harbor, and north to south parallel to the eastern shoreline. Pilot surveys were conducted in the northern part of the southeastern CAD cell near borings FP-03-05 and FP-03-06 where the depths to refusal were 18.5 and 23 m below MLLW, respectively. Chirp data from Profile D, which ran west to east through the middle of the proposed southeastern CAD cell, showed some near-surface subbottom reflections, but no reflections at depth. Most of the signal was reflected off the bottom causing multiples in the record. The data from the analog sources were band-pass filtered to strip out the high-frequency side-echo data and low-frequency noise. Still, there was very little depth of penetration. Even where core data indicated 30 to 41 m of unconsolidated deposits, the seismic data only imaged a few boulders and coarse deposits in the near surface. In general, there were strong reflections off the water bottom, leading to strong multiples in the seismic record. Only limited depth of penetration was achieved with the analog seismic sources. After a preliminary evaluation, it was decided not to collect the rest of the survey lines in the grid, as there was not an improved depth of penetration. Because of the poor data quality of these profiles and their limited value, these profiles are not shown, but were provided to the USACE and are available upon request.

Summary and Conclusions

A marine geophysical investigation was conducted by the U.S. Geological Survey in support of a U.S. Army Corps of Engineers evaluation of the feasibility of locating potential confined aquatic disposal (CAD) cells in Bridgeport Harbor. Three water-based geophysical methods were used to evaluate the geometry and composition of subsurface materials—continuous seismic profiling (CSP), continuous resistivity profiling (CRP), and marine magnetometer surveying. These techniques make use of sound signals, electrical signal propagation, and geomagnetism to interpret the depth to water bottom and bedrock, to evaluate subbottom materials, and to locate large metallic features, such as cables and pipes. All data were located using global positioning systems (GPS), and the GPS data were used for real-time navigation.

This investigation shows the importance of using multiple methods to reduce the ambiguity of the interpretation of the individual methods and strengthen their collective interpretation. In addition, results of corehole sampling were used to ground-truth the data, validate the interpretation of depth to bedrock, and constrain the interpretation of the CRP relative to the drilling and the CSP.

The initial geophysical surveys were conducted over the proposed southwestern CAD cell in April 2006. The initial seismic surveys conducted with the chirp systems produced marginal results with signal penetration of the subbottom only in limited locations. The bedrock surface was imaged in small windows where the seismic signal could penetrate the subbottom, usually in places where channel excavation and maintenance had removed organic materials or loosened the hard bottom. The CSP data were adversely affected by water-bottom multiples. These multiples, which are caused by the presence of entrapped gas in the sediments or by hard sediments, are the records of sound waves that travel multiple times between the water surface and the water bottom. Seismic

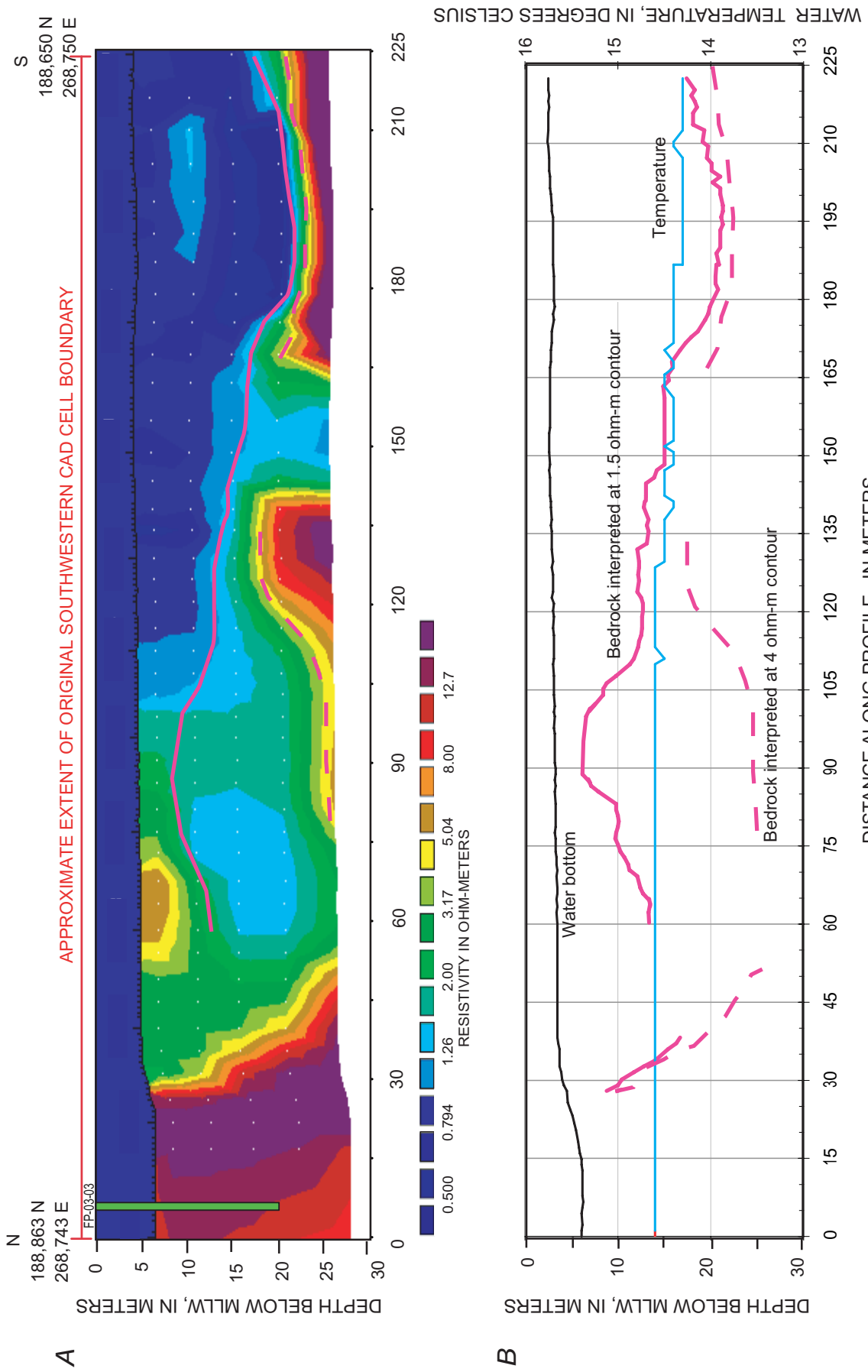

Figure 17. Continuous resistivity survey from Profile B, Bridgeport Harbor, Bridgeport, Connecticut, showing (*A*) the inverted, constrained data, and (*B*) the interpretation of depth to bedrock, measured depth to water bottom, and temperature of near-surface water in degrees Celsius. The solid and dashed red lines show the interpreted bedrock surface. Depths are shown in meters below the mean low-low water (MLLW) surface. The profile runs southwest to northeast. End-point positions are in Connecticut State Plane Coordinate System using the North American Datum of 1983, in meters.

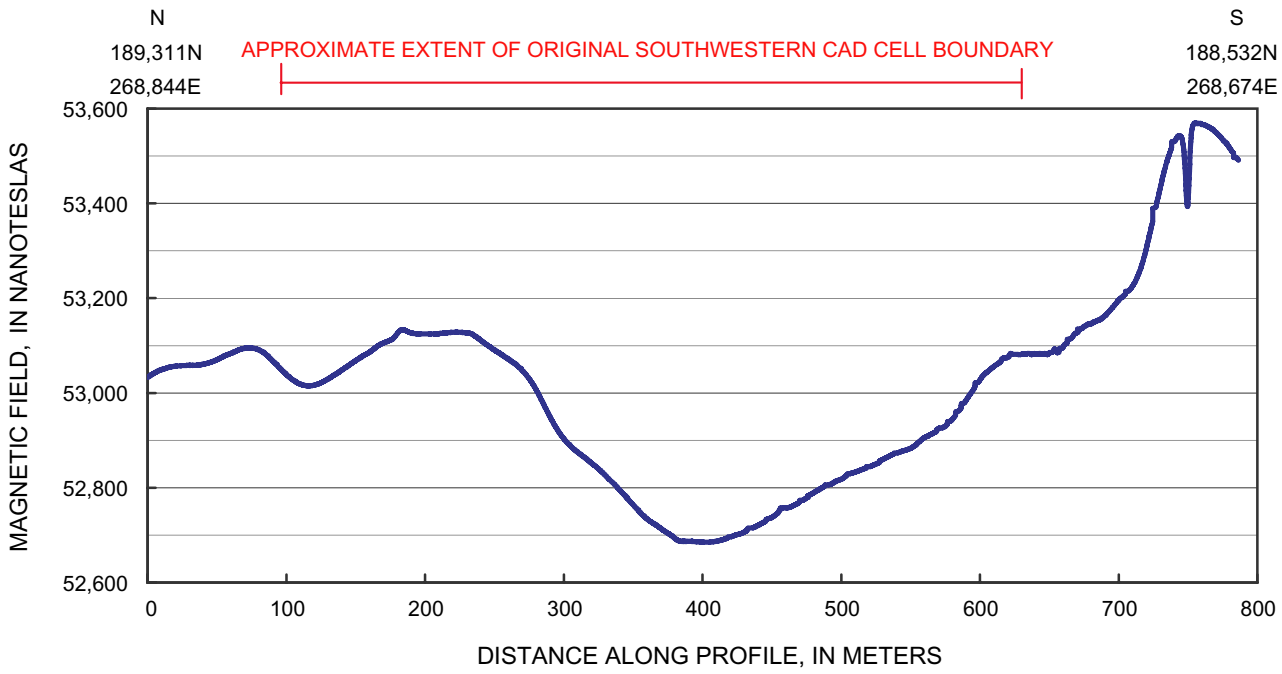

Figure 18. Magnetometer data collected along Profile B, Bridgeport Harbor, Bridgeport, Connecticut. End-point positions are in Connecticut State Plane Coordinate System using the North American Datum of 1983, in meters.

signals that penetrated through the water bottom produced reflections off the bedrock surface. These reflections are characterized by a low-amplitude reflection that typically is irregular and discontinuous. In general, the seismic records indicate that the relief on the bedrock surface is greater than the relief on the surface of the overlying sediments and the water bottom or "mudline" in the harbor. In some locations along the profile, however, the water bottom conforms to the bedrock topography. The greatest depth to bedrock in the geophysical surveys was 42.7 m below mean low-low water (MLLW). This deep reflector was observed on Profile 1 under the navigation channel and was consistent with observations made in boring FP-03-10. A similar reflector could be traced under the southwestern CAD cell along Profile 1 and was interpreted as bedrock. Initial results showed that the depth to bedrock under the southwestern CAD cell was shallow at 8 to 15 m below the water surface. The reflector identified along Profile 1 agreed fairly well with the interpretation of bedrock in boring FB-06-1.

In a pilot study conducted over the proposed southeastern CAD cell in October 2006, different seismic sound source and receiver systems were used to try to improve signal penetration and the quality of the data. The entrapped gas, however, adversely affected these data too, and the depth to bedrock could not be determined. These observations are consistent with boring data and anecdotal information that suggest the water bottom has soft, organic-rich sediments that potentially contain entrapped methane gas that can impede the seismic signal penetration.

Interpretations of the CSP data also were tested for repeatability. In many of the CSP profiles, the same interpretations were obtained, but in a few profiles, the interpretations of the bedrock surface were not repeatable, indicating poor data quality and low confidence in the interpretation. In general, the data were fair to poor quality, as they were adversely affected by the water-bottom multiples.

The CRP record for Profile 1 initially was interpreted using an assumed resistivity contour of 4 ohm-m for the bedrock surface, but that produced a bedrock surface that was deeper than the CSP record. When, bedrock was reinterpreted to be at the 1.2 to 1.5 ohm-m contour in the CRP inversions, results were similar to those interpreted from the CSP records. The crystalline bedrock typically is more resistive than the water-saturated sediments. For this investigation, the saltwater was assumed to have a resistivity of 0.3 to 0.5 ohm-m, and the saltwater-saturated sediments were assumed to have a resistivity of 0.5 to 1.5 ohm-m. The relatively resistive zones associated with seismic reflection locations are interpreted as bedrock. Even with a long electrode spacing of 10 m, the CRP method only imaged a total of about 25 m including the water column. Because of the geometry of the measurement and the inversion, the edges and the deepest zones of the resistivity profiles have the greatest uncertainty. Caution should be used not to overinterpret the data. In general, the CRP data were used to corroborate the CSP interpretations. The shape of the bedrock surface interpreted from the CRP data usually was similar to the bedrock surface imaged in the CSP profiles.

Evaluation of the CRP profiles indicated that the inversions were adversely affected where the depth or ionic

concentration of the water column varied. The models used for these inversions required the water resistivity to be fixed, although the depth of the column could vary. Results indicated that whenever the water depth varied significantly, for instance going into the channel from shallow water, the inversions produced artifacts. Consequently, the CRP profiles were broken into short intervals that extended just over the area of interest, where the depth to the water bottom was fairly constant. Over these short profiles, efforts were made to evaluate the resistivity of the very shallow sediments to determine if there were any large contrasts in resistivity that might indicate differences in the shallow subbottom materials; however, no conclusions could be drawn from the distribution of resistivity in the profiles.

A series of magnetic surveys were conducted in Bridgeport Harbor in April 2006. The magnetic data from Profiles 3, A, and to a lesser extent Profile B, indicate a strong linear magnetic anomaly trending northeast and southwest. This anomaly may represent a large-scale anthropogenic feature. Other isolated anomalies did not appear to be continuous or large scale. These features could be due to topographic changes, changes in the height of the sensor above the bottom, or metallic debris on the bottom or in the subbottom.

The results of interpretation of the CSP, CRP, and magnetometer data are consistent with the conceptual site model of a bedrock channel incised or eroded into sediments and (or) bedrock beneath the present day harbor. The channel appears to follow a north-northwest to south-southeast trend and is parallel to the Pequannock River. The seismic record and boring data indicate that under the channel in the dredged part of the harbor, the depth to bedrock is as deep as 42.7 m below MLLW. The bedrock channel becomes less deep towards the shore, where bedrock outcrops have been mapped at land surface. CSP and CRP data were able to provide a discontinuous, but reasonable, trace from the channel toward the west under the southeastern CAD cell. The CSP and CRP data indicate a high amount of relief on the bedrock surface, as well as along the water bottom. Under the proposed southwestern CAD cell, the sediments are only marginally thick enough for a CAD cell and are about 8 to 15 m thick. Some of the profiles show small diffractions in the unconsolidated sediments, but no large-scale boulders were identified. No bedrock reflectors were imaged under the southeastern CAD cell, where core logs indicate the bedrock is as much as 30 m below MLLW.

References

Breiner, S., 1999, Applications manual for portable magnetometers: San Jose, California, Geometrics, Inc., 58 p. *ftp://geom.geometrics.com/pub/mag/Literature/m-ampm.pdf* (last accessed 24 Jan. 2007)

Day-Lewis, F.D., White, E.A., Belaval, M., Johnson, C.D., and Lane, J.W., Jr., 2006, Continuous resistivity profiling to delineate submarine ground-water discharge—Examples and limitations: The Leading Edge, v. 25, no. 6, p. 724–728.

Edwards, L.S., 1977, A modified pseudosection for resistivity and IP: Geophysics, v. 42, no. 5, p. 1020–1036.

Haeni, F.P., 1986, Application of continuous seismic reflection methods to hydrologic studies: Ground Water, v. 24, no. 1, p. 23–31.

Loke, M.H., 2001, Tutorial—2-D and 3-D electrical imaging surveys: 110 p. *http://www.geoelectrical.com* (last accessed 13 Mar. 2001)

Mackenzie, K.V., 1981, Discussion of sea water sound-speed determinations: Journal of Acoustic Society of America, v. 70, p. 801–806.

Schock, S.G., and LeBlanc, L.R., 1990, Chirp sonar—New technology for sub-bottom profiling: Sea Technology, v. 31, no. 9, p. 35–43.

Smith, Kenneth, 1997, Cesium optically pumped mangetometers—Basic theory of operation: San Jose, Calif., Geometrics, Inc., Technical Report M-TR91, 8 p.

Telford, W.M., Geldart, L.P., and Sheriff, R.E., 1990, Applied geophysics (2nd ed.): New York, Cambridge University Press, 770 p.

Trabant, P.K., 1984, Applied high-resolution geophysical methods: Boston, International Human Resources Development Corporation, 265 p.

U.S. Army Corps of Engineers, 2004, Corpscon, version 6.x, technical documentation and operating instructions: Alexandria, Va., U.S. Army Corps of Engineers, Engineer Research and Development Center, Topographic Engineering Center, 29 p.

Ward, S.H., 1990, Resistivity and induced polarization methods, *in* Ward, Stanley, ed., Geotechnical and environmental geophysics no. 5: Tulsa, Okla., Society of Exploration Geophysicists, p. 147–190.

Zohdy, A.A.R., Eaton, G.P., and Mabey, D.R., 1974, Application of surface geophysics to ground-water investigations: U.S. Geological Survey Techniques of Water-Resources Investigations, book 2, chap. D1, 116 p.